BRL

AD

REPORT NO. 1322

THE VARR METHOD

A TECHNIQUE FOR DETERMINING THE EFFECTIVE POWER PATTERNS OF MILLIMETER-WAVE RADIOMETRIC ANTENNAS

by

R. B. Patton, Jr.
C. L. Wilson

May 1966

U. S. ARMY MATERIEL COMMAND
BALLISTIC RESEARCH LABORATORIES
ABERDEEN PROVING GROUND, MARYLAND

Destroy this report when it is no longer needed.
Do not return it to the originator.

The findings in this report are not to be construed as an official Department of the Army position, unless so designated by other authorized documents.

The use of trade names or manufacturers' names in this report does not constitute indorsement of any commercial product. They are included for the sole purpose of permitting the reader to evaluate the experiments.

B A L L I S T I C R E S E A R C H L A B O R A T O R I E S

REPORT NO. 1322

MAY 1966

THE VARR METHOD

A TECHNIQUE FOR DETERMINING THE EFFECTIVE POWER PATTERNS OF MILLIMETER-WAVE RADIOMETRIC ANTENNAS

R. B. Patton, Jr.
C. L. Wilson

Ballistic Measurements Laboratory

RDT&E Project No. 1P523801A286

A B E R D E E N P R O V I N G G R O U N D, M A R Y L A N D

B A L L I S T I C R E S E A R C H L A B O R A T O R I E S

REPORT NO. 1322

RBPatton,Jr/CLWilson/cr
Aberdeen Proving Ground, Md.
May 1966

THE VARR METHOD

A TECHNIQUE FOR DETERMINING THE EFFECTIVE POWER PATTERNS OF MILLIMETER-WAVE RADIOMETRIC ANTENNAS

ABSTRACT

The VARR (VAriable Range Reflector) Method is a technique which has been developed to measure the effective power patterns of millimeter-wave radiometric antennas. In this method, a large movable metallic surface is oriented to reflect radiation from the zenith into an antenna which is directed along the horizontal. Radiometric temperature is measured as a function of the range of the reflector from the antenna. In addition, the water vapor content of the atmosphere and the radiometric temperatures in the directions of background and zenith are observed.

A computing procedure has been devised to determine the complete pattern and gain characteristics of the antenna system purely on the basis of data provided by the measuring system. The method has been used to successfully determine the effective power patterns of a number of antenna systems. These results form the basis of a comparative evaluation of antenna system performance that is in substantial agreement with the observed effectiveness of these same antennas in previous measurements.

TABLE OF CONTENTS

LIST OF SYMBOLS

SYMBOLS

a	fractional power loss in the atmosphere
b	a fitted parameter which characterizes the central portion of the pattern
h	height of the background above the level of the antenna, ft
r	radius of the assumed circular reflector, yds
B	fitted background temperature, ^{o}K
C	matrix of coefficients of least-squares equations of condition
D	diameter of antenna aperture, in.
G	the antenna gain function
G_o	the antenna gain, power
I	the integral $\int G(\theta) \sin \theta \, d\theta$
R	range of the reflector from the antenna, yds
S	side of the assumed square reflector, yds
T	temperature, ^{o}K
V	column matrix with elements ln T_i
X	column matrix with elements ln B and b
α	angular distance from antenna axis, deg
β	fractional loss in rf system, power
ϵ	elevation angle measured from antenna site, deg
η	an angle defined by Equation (A3)
θ	angular distance from antenna axis, deg
λ	operating wavelength of the radiometric antenna, ft
ρ	range from antenna to beginning of far-field, yds
ϕ	azimuthal angle about antenna axis, deg
ψ	an angle defined by Equation (27)

SUBSCRIPTS

i	index for measurements and related quantities pertaining to central portion of the beam
j	index for measurements and related quantities pertaining to the side of the beam
k	summation index
n	maximum value of index i
o	identifies quantities where either i or j are zero
t	refers to theoretical values
B	refers to background
M	specifies measured temperatures
N	minimum value of index j
Z	refers to zenith
W	refers to rf system
MB	specifies measured background temperature
MZ	specifies measured zenith temperature

SUPERSCRIPTS

*	Identifies quantities associated with assumed square reflector
-	identifies quantities associated with the point that establishes the set of measurements to fit to Equation (12)
1	identifies transposed matrices

INTRODUCTION

An investigation of the application of radiometric techniques to the problem of acquisition and guidance of close-to-ground targets led to a study of the optimization of antenna systems for radiometers. Most antennas will receive signals from outside the main beam; in the radiometric application, the entire background radiates into that part of the receiving pattern which is not incident on the target. The signal contrast between the target and the background is considerably decreased by this extraneous background signal. In order to establish the system receiving sensitivity to the target as a function of range and the pointing accuracy of the system, it is necessary to know the effective power pattern and the gain of the antenna as used in the radiometric system environment.

Unexpectedly wide variations were encountered in the radiometric performance of antennas with similar apertures. These results prompted an investigation of methods for measuring complete pattern and gain characteristics of non-coherent, narrow beam antenna systems. Conventional methods, employing a coherent source, require a prohibitive number of difficult measurements. Therefore, the VARR (VAriable Range Reflector) method was devised for the comparative evaluation of antenna systems. In this method, a single series of simple measurements of the total energy received by a particular antenna provides sufficient information to completely determine these characteristics.

The VARR method requires a large movable metallic surface so oriented as to reflect radiation from the zenith into the antenna of a radiometer. A series of measurements are obtained with the antenna directed along a horizontal path toward the center of the reflector. Observations of radiometric temperature are recorded as a function of the range of the reflector from the antenna. In addition, measurements of temperatures in the directions of the background and zenith are made.

The effective power pattern of the antenna is determined by a computing procedure which has been derived from a simple geometrical model that closely approximates the actual geometry of the system. On the basis of this model and several simplifying assumptions, the measured radiometric temperature has been expressed as a function of the background and zenith temperatures, the range of the reflector from the antenna, and the effective power pattern of the antenna. Computing procedures have been devised to use this function and the measured temperatures to determine both the pattern and the gain of the antenna.

Effective power patterns have been computed for several antennas by the VARR method. In general, the results have indicated a somewhat broader beam than was indicated by coherently measured patterns for these same antennas. Field comparison measurements of the performance of these antennas tend to show that radiometer antenna performance can be predicted from these effective power patterns.

SECTION I

THE VARR MEASURING TECHNIQUE

A technique for measuring effective power patterns in a real environment for antenna comparison purposes has been devised. The method makes use of a large movable reflector (Figure 1) positioned at a fixed elevation angle of 45° to reflect the cold zenith temperature into the radiometer antenna. Measurements are made with the radiometer antenna pointed along a horizontal path to the center of this reflector while the reflector is moved horizontally along the ground to change the distance between the antenna and the reflector.

At close range the large reflector intercepts the total antenna beam and the measured radiometric temperature equals the zenith temperature. As the distance between the antenna and the reflector is increased, the reflector intercepts less and less of the beam and the measured temperature approaches the temperature of the background. By choosing a suitable background with a nearly constant temperature, such as a hill or high vegetation, the measured temperature is proportional to the ratio of the total antenna beam angle to the reflector interception angle.

Antennas of various types including parabolas, plano-convex plastic lenses, and plastic Fresnel-zone plates were measured with radiometers operating at 35, 68.5, 94, and 140 Gc. The precision of these measurements was limited to plus or minus one degree Kelvin by the radiometer sensitivity.

The flat-sheet aluminum reflector was 16 feet high, 12 feet wide, and tilted at an angle of 45° with the horizontal. This gave an effect flat-plate area of approximately 136 square feet.

The background consisted of trees 60 feet in height at a range of approximately 1800 feet for the low frequency measurements and 6500 feet for the higher frequencies. The measured radiometric temperature of this background was close to ambient when the reflector was not in the beam. The ground surface between the reflector and the antenna was covered with a 6 inch growth of grass and weeds.

At the start of each run the reflector was moved in very close to the antenna to intercept the maximum portion of the antenna capture area. A measurement of radiometric temperature in the direction of the zenith was compared with the reflected radiometric zenith temperature. No measureable difference could be detected between these two measurements if the aluminum reflector was periodically washed to keep the surface clean.

The reflector was then moved horizontally away from the antenna in successive steps. The temperature was measured with the antenna pointing at the center of the reflector at each position. The plots in Figures 5, 7, 9, 11, 13, 15, 17, and 19 show these measured temperatures versus range. At the end of each run the background temperature was again measured to ascertain if any change had occured in atmospheric conditions which could affect the measurement. A feeling of confidence in the precision of the data developed when the curves obtained by means of this method were reasonably smooth and repeatable.

SECTION II

VARR COMPUTING METHODS

Approach to the Problem

To determine the effective power pattern of an antenna by the VARR method of measurement, it is convenient to divide the computing procedure into two separate, but related parts. In the first of these, the pattern at and near the center of the beam is obtained by fitting an exponential function of second degree to those measurements of temperature which were made with the reflector at its more remote positions from the antenna. This requires a computation to determine two parameters which are nonlinear functions of the measured temperatures. The second phase of the data reduction procedure consists of a series of computations which are designed to determine the remainder of the pattern, section by section, while constraining all segments of the fitted curve to join continuously. The method has been found to be practical for reflectors of various geometrical shapes. In particular, a simplified solution yielding sufficiently accurate results may be obtained if the reflector is assumed to be a circular disk normal to the antenna axis and subtending the same solid angle as the actual reflector. It will be shown that the errors resulting from the circular approximation are well within the limits imposed by the accuracy requirements. The results are generally considered to be useful if the overall errors do not exceed 15 percent. Moreover, corrections will be derived to compensate for those errors which do arise from the circular approximation for the reflector. While the derivations are rather involved, the resulting corrections are small enough to neglect entirely, but are very easy to apply when greater accuracy is desired.

Fundamental Equation

To simplify a portion of the derivation of the computing method, attenuation will be neglected initially and introduced later at a convenient point in the development. In the absence of significant attenuation

and assuming the reflector to be in the far-field of the antenna, the computing procedures are based upon the following expression for the measured temperature T_M:

$$T_M = \frac{\int_0^{2\pi} \int_0^{\pi} T(\theta,\phi)G(\theta,\phi) \sin\theta \, d\theta \, d\phi}{\int_0^{2\pi} \int_0^{\pi} G(\theta,\phi) \sin\theta \, d\theta \, d\phi} . \qquad (1)$$

The symbols θ and ϕ are angles which specify a direction with respect to the antenna. Thus, (θ, ϕ) is defined to be the direction whose angular distance from the antenna axis is θ and whose azimuthal position about the axis is given by ϕ · T (θ,ϕ) is the temperature and G (θ, ϕ) is the value of the gain function in the direction (θ,ϕ).

We desire to determine G (θ,ϕ) in Equation (1) from a series of temperature observations for various ranges of the reflector. Our development ispredicated upon several simplifying assumptions which closely approximate the actual physical situation. In the initial treatment of Equation (1), we will assume the reflector to be a circular disc normal to the antenna axis and subtending a solid angle equal to that subtended by the actual reflector. The background will be considered to radiate at the constant temperature T_B and the disk at the constant temperature T_Z, the equivalent of the reflected zenith temperature. We will limit our discussion to antennas with patterns that are symmetrical about their axes. Purely as a matter of convenience, we add the further restriction that for $\theta > \frac{\pi}{2}$, G (θ) = 0. Introducing the usual constraint that

$$\frac{1}{4\pi} \int_0^{2\pi} \int_0^{\pi} G(\theta,\phi) \sin\theta \, d\theta \, d\phi = 1 , \qquad (2)$$

Equation (1) may be written as

$$T_M(\alpha) = 1/2 \left(T_Z I_o^{\alpha} + T_B I_{\alpha}^{\frac{\pi}{2}} \right), \tag{3}$$

where α is defined to be the angle between the axis of the antenna and any line from the center of the antenna to the edge of the circular disk. The symbol I_e^f is defined by the definite integral

$$\int_e^f G(\theta) \sin \theta \, d\theta \, .$$

In particular, we note that

$$I_o^{\alpha} + I_{\alpha}^{\frac{\pi}{2}} = 2. \tag{4}$$

Justification of Assumptions

The development of Equation (3) has been predicated upon certain simplifying assumptions that require justification. These assumptions are:

1. the source for temperature T_z is a circular disk normal to the antenna axis,
2. the background temperature is constant,
3. the reflector is in the far-field of the antenna,
4. there is no significant attenuation of the received radiation.

In regard to the first assumption, the reflector was in fact a rectangle inclined at an angle of 45° to the axis of the antenna so as to reflect the zenith temperature. The dimensions of the rectangle were such that its component normal to the axis of the antenna approximated a square. It will be shown later, after further mathematical development, that a target consisting of a circular disk normal to the antenna axis with an area equal to that of the square and radiating at a temperature T_Z constitutes an excellent approximation to the actual physical situation. Moreover, the accuracy of the results for the circular approximation can be significantly improved by relatively simple corrections which also will be derived.

The assumption of constant background temperature will be satisfied only if that portion of the background consisting of sky has a negligible effect on the temperature measurement. The VARR method of pattern determination has been used at 35 Gc, 68.5 Gc, and higher frequencies. In Figure 2, radiometric temperatures are plotted as a function of the elevation angle for three frequencies. We note that for the two higher frequencies, there is no appreciable change in the measured temperature for the first 100 mils in elevation. This results primarily from the radiation of the relatively thick layer of the lower atmosphere. Hence, with narrow beam antennas operating at frequencies of 68.5 Gc and above, the nonhomogeneous background does, indeed, have a negligible effect and the assumption of a constant background temperature is quite valid. However, to add a factor of safety, the measurements for pattern determinations at these higher frequencies were made against a background of trees, approximately 60 feet in height and located 6500 feet from the antenna. For the 35 Gc frequency, where the variation of measured temperature with elevation angle is much greater, the distance between the background of trees and the antenna was reduced to 1800 feet. Thus, with the antenna 8 feet above the ground, the background subtended an angle of 1.7° at the instrumentation site. In Appendix A it is shown that with this geometry, the variation in background temperature contributes no error to the determination of that portion of the pattern within 1.7° of the antenna axis. Moreover, with a narrow beam, the errors in the determination of the remainder of the pattern will be negligible.

The assumption that the reflector is in the far-field of the antenna is obviously not valid for the entire set of measurements since a number of the temperature observations were made with the reflector close to the antenna. On the other hand, it is clear that a portion of the data has been obtained with the reflector unquestionably in the far-field of the antenna. Moreover, the reduction procedure is designed to initially determine the central portion of the pattern, and from it the gain of the antenna, on the basis of observations that are taken with the reflector definitely in the far-field. The remainder of the pattern is computed section by section from observations considered in pairs and used in

the order of decreasing range. Hence, if Equation (1) becomes invalid for a portion of the observations, only the sides of the pattern will be affected while the determination of the central portion of the beam remains free of any error resulting from the use of this simplifying assumption. A portion of the sides of the pattern is determined from data obtained while the reflector is in the near-field. Hence, this portion of the effective power pattern is not completely representative of the free space side-lobes. However, no abrupt discontinuity occurs as the range to the reflector is decreased and this gradual transition is further smoothed because at the closer range, the reflector is much larger than the main beam. The dashed portions of the computed patterns (Figures 6, 8, 10, 12, 14, 16, 18, and 20) indicate the region in question. The total computed power patterns are given for comparison purposes.

The fourth and last assumption, of no significant attenuation was convenient for the derivation of Equation (3). However, the effect of attenuation is frequently significant and should be taken into account . Therefore, the previous development will be expanded to include this effect in both the atmosphere and the radio frequency (rf) system.

Treatment of Attenuation

We consider the terms a and β which are defined to be the fractional power losses in the atmosphere and the rf system respectively. The atmosphere is assumed to be at a molecular temperature equivalent to the background temperature T_B while the average temperature of the lossy elements of the system are denoted by T_W. Introducing both attenuation terms into Equation (3) yields

$$T_M(\alpha) = \left[\frac{1-\beta}{2}\right]\left[\left\{(1-a)T_Z + aT_B\right\}I_o^{\alpha} + T_B I_{\alpha}^{\frac{\pi}{2}}\right] + \beta T_W, \qquad (5)$$

where it is to be understood that the term a is a function of the range of the reflector which is the source of the temperature T_Z. With the

aid of Equation (4), we may write

$$T_M(\alpha) = 1/2\left[(1 - \beta)T_Z + a(1 - \beta)(T_B - T_Z) + \beta T_W\right]I_o^{\alpha} + 1/2\left[(1 - \beta)T_B + \beta T_W\right]I_{\alpha}^{\frac{\pi}{2}} . \quad (6)$$

Of particular interest are the quantities T_{MB} and T_{MZ} which are defined to be the measured background and zenith temperatures respectively. The temperature measurement T_{MB} is obtained with the antenna oriented horizontally and the reflector entirely removed from the field of view of the antenna. Since it has been assumed that the background temperature T_B is equivalent to the ambient temperature, we conclude that

$$T_{MB} = (1 - \beta)T_B + \beta T_W . \quad (7)$$

The measured zenith temperature may be obtained by either one of two completely equivalent procedures. First, the antenna simply is directed along the vertical. In the second method, it is aligned horizontally with the reflector placed immediately adjacent so as to capture the entire beam of the antenna. Both methods have been observed to yield identical results. We note that

$$T_{MZ} = (1 - \beta)T_Z + \beta T_W . \quad (8)$$

It should, perhaps, be observed that T_Z is not the sky temperature, but rather the temperature which results from viewing the sky through the atmosphere whereas T_{MZ} is the actual recorded observation. Combining Equations (7) and (8), it may be established that

$$(T_{MB} - T_{MZ}) = (1 - \beta)(T_B - T_Z) . \quad (9)$$

Substituting Equations (7), (8), and (9) into Equation (6) yields

$$T_M(\alpha) = 1/2\left[\left\{T_{MZ} + a(T_{MB} - T_{MZ})\right\}I_o^{\alpha} + T_{MB}I_{\alpha}^{\frac{\pi}{2}}\right] , \quad (10)$$

which, with the aid of Equation (4) can be simplified to

$$T_M(\alpha) = T_{MB} - 1/2(1 - a)(T_{MB} - T_{MZ})I_o^{\alpha} . \qquad (11)$$

We have now derived an expression for the measured temperature in terms of the atmospheric fractional loss, which varies with range, the angle subtended by the reflector, the gain function of the antenna, and the measured zenith and background temperatures. Let us emphasize that, while Equation (11) pertains to the far-field, it is valid over a sufficient range of α to clearly establish the character of the effective power pattern of the antenna.

Computing Methods for a Circular Reflector

The first phase of the computing procedure for determining the pattern consists of fitting a curve to those temperature measurements which pertain to the central portion of the beam. Since temperature is recorded as a function of the range of the reflector, the measured temperature approaches the background temperature as the range increases (Figures 5, 7, etc.), i.e., as α decreases and approaches zero. This suggests the possibility of fitting an exponential curve to those temperature measurements obtained with the reflector at its more remote positions from the antenna. Indeed, it has been found for all measurements to date that it is possible to fit the observations to a curve of the form

$$T(\alpha) = Be^{-b\alpha^2} , \qquad (12)$$

for α in the interval $(o,\bar{\alpha})$. If the assumed circular reflector is at a range R from the radiometer and has a radius of r, we note that

$$\alpha = \tan^{-1}(r/R) . \qquad (13)$$

The terms $\bar{\alpha}$, B, and b are parameters which may be evaluated by the least squares fitting procedure which is presented in Appendix B. The parameter B constitues the fitted value for the background temperature. Combining Equations (11) and (12) while replacing T_{MB} with its improved value B

and restricting α to be equal to or less than $\bar{\alpha}$, we obtain

$$Be^{-b\alpha^2} = B - 1/2(1 - a)(B - T_{MZ})I_o^{\alpha} . \tag{14}$$

The attenuation term a is a function of R, the range of the reflector. To simplify the problem, we approximate the term a by a_o, its average value for those measurements fitted to the curve specified by Equation (12). Both sides of Equation (14) may be differentiated with respect to α and solved for $G(\alpha)$ to obtain

$$G(\alpha) = \left[\frac{4bB}{(B - T_{MZ})(1 - a_o)}\right]\left[\frac{\alpha}{\sin \alpha}\right]e^{-b\alpha^2} . \tag{15}$$

The parameter $\bar{\alpha}$, which is determined by means of the fitting procedure, is sufficiently small that, for $\alpha \leq \bar{\alpha}$, sin α may be approximated by α. Hence, Equation (15) reduces to

$$G(\alpha) = \left[\frac{4bB}{(B - T_{MZ})(1 - a_o)}\right]e^{-b\alpha^2} . \tag{16}$$

Defining G_o to be the gain of the antenna, we observe that

$$G_o = G(o) = \frac{4bB}{(B - T_{MZ})(1 - a_o)} . \tag{17}$$

We have now established that, in the vicinity of the center of the beam where $\alpha \leq \bar{\alpha}$, the effective power pattern of the antenna is well approximated by

$$G(\alpha) = G_o e^{-b\alpha^2} . \tag{18}$$

It has been found impractical to determine $G(\alpha)$ for $\alpha > \bar{\alpha}$ by curve fitting procedures. The measured data for this portion of the pattern generally do not conform to a single type of curve, but vary considerably from run to run. We determine the remainder of the pattern by a less rigorous approach in which $G(\alpha)$ is approximated by a step function for $\alpha > \bar{\alpha}$. The midpoints of each step are assumed to be discrete points of the pattern. These, together with Equation (18) determine the pattern

over the complete range of α, or at least for all values of α up to the point where Equation (11) is no longer valid as a result of the reflector being no longer in or near the far-field.

The initial step in this phase of the reduction procedure consists of plotting the measured temperature as a function of the range R for the interval $(0, \bar{R})$, $\bar{R}$ being the range which corresponds to the angle $\bar{\alpha}$. Referring to Equation (13), we note that

$$\bar{R} = r \cot \bar{\alpha}. \tag{19}$$

In addition, Equations (12) and (13) are used to compute the fitted temperature as a function of range and this curve is then plotted for $R \geq \bar{R}$. A smooth curve is drawn to fit the points plotted in the interval $(0, \bar{R})$ while constraining it to join the previously fitted curve at a point where $R \geq \bar{R}$ in such a way that the two segments form a continuous curve and have identical slopes at the point where they join. Let the values of R and α at this point be given by R_o and α_o respectively. Temperatures are read from the curve for several values of R within the interval $(0, R_o)$. Let these temperatures and corresponding ranges be denoted respectively by T_j and R_j where $j = 0, 1, 2, \ldots, N$ with the condition that

$$R_N < R_{N-1} < \ldots R_2 < R_1 < R_o.$$

The term α_j is defined as the value of α corresponding to the range R_j so that

$$\alpha_j = \tan^{-1}(r/R_j). \tag{20}$$

We assume that $G(\alpha)$ can be approximated by a step function that changes values on the discrete set of discontinuities defined by α_j. Let $G_{j\,(j+1)}$ be the value of the function over the interval $(\alpha_j, \alpha_{(j+1)})$. Referring to Equations (11) and (18) with T_{MB} replaced by B, we relate

the temperatures T_j to the step function approximating G (α) for j = 1, 2, ..., N by the expression

$$T_j = B - 1/2(1 - a_j)(B - T_{MZ})\left[\int_o^{\alpha_o} G_o e^{-b\theta^2} \sin\theta\, d\theta + \sum_{k=o}^{(j-1)} \int_{\alpha_k}^{\alpha(k+1)} G_{k(k+1)} \sin\theta\, d\theta\right], \quad (21)$$

and for j = 0 by the expression

$$T_o = B - 1/2(1 - a_o)(B - T_{MZ}) \int_o^{\alpha_o} G_o e^{-b\theta^2} \sin\theta\, d\theta. \quad (22)$$

The terms b, B, and G_o are obtained from the fitting procedure for the central portion of the beam while a_j is the value of the attenuation term for the reflector at the range R_j. With j = 1, we may combine Equations (21) and (22) to obtain

$$G_{o1} = \frac{2}{(B - T_{MZ})(\cos\alpha_o - \cos\alpha_1)}\left[\frac{B - T_1}{1 - a_1} - \frac{B - T_o}{1 - a_o}\right], \quad (23)$$

and, in general, we have

$$G_{j(j+1)} = \frac{2}{(B - T_{MZ})(\cos\alpha_j - \cos\alpha_{(j+1)})}\left[\frac{B - T_{(j+1)}}{1 - a_{(j+1)}} - \frac{B - T_j}{1 - a_j}\right]. \quad (24)$$

The step function was used as an aid to integration. We now replace the step function by a series of discrete points and assume that $G_{j(j+1)}$ is the value of G (α) for $\alpha = \alpha_{j(j+1)}$ where

$$\alpha_{j(j+1)} = 1/2\left(\alpha_j + \alpha_{(j+1)}\right). \quad (25)$$

Our solution for the effective power pattern of the antenna then consists of the exponential function given by Equation (18) over the interval $(0,\alpha_o)$ and a curve segment joining the exponential function and passing through the discrete points $(\alpha_{j(j+1)}, G_{j(j+1)})$. These descrete points are computed in sufficient number to establish the character of the pattern on either side of the central portion of the beam.

Corrections for the Circular Approximation

In the development thus far, the reflector has been assumed to be a circular disk normal to the antenna axis when in fact, it was a rectangular surface so oriented as to appear approximately square when viewed from the position of the antenna. Therefore, in this portion of the development, let us assume the reflector to be a square normal to the axis of the antenna. The errors resulting from this assumption are trivial and may be safely ignored. However, it will shortly be shown that the errors resulting from the assumption of a circular reflector are small, but not negligible. Moreover, expressions will be derived for the evaluation of these errors and in the process, corrections for the previous development will be determined.

Let us first develop an expression for the measured temperature when the reflector is approximated by a square with sides of length S. As before, we assume a constant zenith temperature T_Z and constant background temperature T_B. Neglecting power lost to the atmosphere and antenna system for the moment, we conclude from Figure 3 that

$$T(R) = \frac{8T_Z \int_0^{\frac{\pi}{4}} \int_0^{\psi} G^*(\theta) \sin\theta \, d\theta \, d\phi + 8T_B \int_0^{\frac{\pi}{4}} \int_{\psi}^{\pi} G^*(\theta) \sin\theta \, d\theta \, d\phi}{\int_0^{2\pi} \int_0^{\pi} G^*(\theta) \sin\theta \, d\theta \, d\phi}, \quad (26)$$

where

$$\psi = \tan^{-1}\left[\frac{S \sec\phi}{2R}\right], \quad (27)$$

and $G^*(\theta)$ is a gain function which is to be evaluated on the basis of a square reflector. Referring to the constraint imposed by Equation (2) and adjusting the limits of integration in Equation (26) to a more

convenient form, we obtain

$$T(R) = T_B - \frac{2\left(T_B - T_Z\right)}{\pi} \int_0^{\frac{\pi}{4}} \int_0^{\psi} G^*(\theta) \sin\theta \, d\theta \, d\phi \, . \qquad (28)$$

Introducing terms to account for power losses to both the atmosphere and the antenna system yields

$$T_M(R) = (1 - \beta) \left[T_B - \frac{2}{\pi}(1 - a)(T_B - T_Z) \int_0^{\frac{\pi}{4}} \int_0^{\psi} G^*(\theta) \sin\theta \, d\theta \, d\phi \right] + \beta T_w . \qquad (29)$$

Expressions derived from Equation (29) for the measured background and zenith temperatures are identical with Equations (7) and (8). With the aid of these we conclude that

$$T_M(R) = T_{MB} - \frac{2}{\pi}(1 - a)(T_{MB} - T_{MZ}) \int_0^{\frac{\pi}{4}} \int_0^{\psi} G^*(\theta) \sin\theta \, d\theta \, d\phi \, . \qquad (30)$$

The angles α_j, defined by Equation (20), determine a family of cones whose common axis passes through the center of the reflector and coincides with the extension of the symmetry axis of the antenna. Consider initially the cone defined by the angle α_o. It has been established for the circular approximation that the antenna pattern is of the form of Equation (18) for $\alpha \ll \alpha_o$ where $\alpha_o \ll \bar{\alpha}$. This corresponds to the condition that $R \gg R_o \gg \bar{R}$. For the development which follows, let R_o^* be a sufficiently large value of the range so that, for $R \geq R_o^*$, the reflector is completely contained within the cone defined by α_o. It follows that the limit of integration ψ in Equation (30) will then be less than α_o. While the function $G^*(\theta)$ in the same equation has not been determined, our previous results for the circular approximation suggest that a curve of the type defined by Equation (18) may be satisfactory. Therefore, let us assume that for $R \geq R_o^*$

$$G^*(\theta) = G_o^* e^{-b^* \theta^2} . \qquad (31)$$

Replacing T_{MB} by its fitted value and combining Equations (30) and (31) yield

$$T_M(R) = B - \frac{2}{\pi}(1 - a)(B - T_{MZ}) \int_0^{\frac{\pi}{4}} \int_0^{\psi} G_o^* e^{-b^* \theta^2} \sin \theta \, d\theta \, d\phi. \quad (32)$$

Since α_o is small and $\psi < \alpha_o$, we may approximate sin θ by θ and ψ by $(\frac{S}{2R})$ sec ϕ. Equation (32) then may be integrated to obtain

$$T_M(R) = B - \frac{(1 - a)(B - T_{MZ})}{b^* \pi} \int_0^{\frac{\pi}{4}} G_o^* \left\{ 1 - e^{-b^* \left(\frac{S \sec \phi}{2R} \right)^2} \right\} d\phi \, . \quad (33)$$

Substituting the first three terms of the series expansion for the exponential and integrating once more yield

$$T_M(R) = B - \frac{G_o^* S^2 (1 - a)(B - T_{MZ})}{4\pi R^2} \left(1 - \frac{b^* S^2}{6R^2} \right) . \quad (34)$$

It follows from the definition of R_o^* that we are considering a range of α for which Equation (12) is valid. Moreover, α is sufficiently small that we may approximate it by r/R and replace the exponential in Equation (12) by the first three terms of the series expansion. Thus,

$$T(R) = B \left[1 - b(\frac{r}{R})^2 + 1/2 \, b^2 (\frac{r}{R})^4 \right]. \quad (35)$$

Recalling that r was defined to be the radius of the assumed circular reflector whose area approximates that of a square with sides of length S, we note that

$$r = S/\sqrt{\pi} \, . \quad (36)$$

Combining Equations (35) and (36) yield

$$T(R) = B - \frac{BbS^2}{\pi R^2} \left(1 - \frac{bS^2}{2\pi R^2} \right), \quad (37)$$

We conclude that the fitted temperatures given by Equation (37) will be equal to the measured temperatures of Equation (34) if

$$\frac{b^* S^2}{6R^2} = \frac{bS^2}{2\pi R^2} \quad ,$$

and

$$\frac{G_o^* S^2 (1 - a_o)(B - T_{MZ})}{4\pi R^2} = \frac{BbS^2}{\pi R^2} \quad ,$$

where the term a has been replaced by an average value a_o. With $R \leq R_o^*$, these two conditions will be satisfied identically if

$$G_o^* = \frac{4bB}{(B - T_{MZ})(1 - a_o)} = G_o \quad ,$$

and

$$b^* = \frac{3}{\pi} b = 0.955b \quad ,$$

so that

$$G^*(\alpha) = G_o e^{-(0.955b)\alpha^2} \tag{38}$$

Comparing Equations (18) and (38), we conclude that the antenna pattern determined for the central portion of the beam with the assumption of a circular reflector will yield better results if the parameter b is multiplied by the factor $(3/\pi)$. This constitutes a correction of approximately 5% in the exponent of Equation (18), but considerably less on the average in $G(\alpha)$ over that range of α for which the equation is a valid approximation to the effective power pattern of the antenna.

In considering the effect of the circular approximation on the remainder of the pattern, it will be convenient for the sake of simplifying the integration, to assume as before that $G^*(\alpha)$ can be approximated by a step function when $R < R_o^*$. The reflector will again be considered to be a square oriented normal to the antenna axis. We define $G^*_{j(j+1)}$ to be the value of $G^*(\alpha)$ on the interval $(\alpha_j^*, \alpha^*_{(j+1)})$. To simplify the mathematical analysis in determining an expression for $G^*j(j+1)$ we limit the range of R so that for $R_j^* \leq R \leq R_{(j+1)}$, the reflector is completely contained within the cone defined by $\alpha^*_{(j+1)}$ while the intersection of the cone defined by α^*_j with the square approximating the reflector is a circle completely contained within the square

(Figure 4). With these restrictions and the aid of Equation (30), the temperature may be expressed as a function of range by

$$T(R) = B - \frac{2}{\pi}(1 - a)\left(B - T_{MZ}\right)\int_{o}^{\frac{\pi}{4}}\left[\int_{o}^{\alpha^*_j} G^*(\theta)\sin\theta\, d\theta + \int_{\alpha^*_j}^{\psi} G^*_{j\,(j+1)}\sin\theta\, d\theta\right]d\phi. \tag{39}$$

To obtain an expression for $G^*_{j\,(j+1)}$, it is convenient to differentiate Equation (39) with respect to R. While the term a is a function of R, it changes so slowly with a change of range that its effect is of second order. Therefore, it will be considered constant with the result that

$$\frac{dT}{dR} = \frac{(1 - a)(B - T_{MZ})S^2 G^*_{j\,(j+1)}}{2\pi}\int_{o}^{\frac{\pi}{4}}\frac{\sec^2\phi}{\left(R^2 + \frac{S^2}{4}\sec^2\phi\right)^{3/2}}d\phi\,. \tag{40}$$

Integrating Equation (40) and then solving for $G^*_{j(j+1)}$, we obtain

$$G^*_{j(j+1)} = \left[\frac{2\pi(R^2 + S^2/4)\sqrt{R^2 + S^2/2}}{S^2(1 - a)(B - T_{MZ})}\right]\frac{dT}{dR}\,. \tag{41}$$

It is desirable to minimize the intervals $(\alpha^*_j, \alpha^*_{(j+1)})$ over which the step function remains constant while observing the assumptions which led to Equation (39). That is to say, when the reflector is at the range $R^*_{(j+1)}$, we desire the cones defined by α^*_j and $\alpha^*_{(j+1)}$ to interesect the plane containing the assumed square reflector in circles which respectively are inscribed in and circumscribed about the square.

This may be accomplished for all values of j by defining R_j^* and α_j^* in terms of R_o^* as follows

$$R_j^* \equiv R_o^*/(\sqrt{2})^j \quad , \tag{42}$$

$$\alpha_j^* \equiv \tan^{-1}\left(\frac{S(\sqrt{2})^{j-1}}{R_o^*}\right) . \tag{43}$$

The last two equations may be combined to obtain

$$\tan \alpha_j^* = \frac{S/2}{R_{(j+1)}^*} , \tag{44}$$

$$\tan \alpha_{(j+1)}^* = \frac{(S/2)\sqrt{2}}{R_{(j+1)}^*} . \tag{45}$$

Hence, the desired conditions have been satisfied. Since this method has been developed for application to very narrow beam antennas with the reflector in or near the far-field, the angle α will normally be sufficiently small that Equation (45) may be written as

$$R_{(j+1)}^* = \frac{S}{\alpha_{(j+1)}^* \sqrt{2}} , \tag{46}$$

and we conclude that R is very much larger than S. Therefore, with the reflector at range $R_{(j+1)}^*$, we may simplify Equation (41) to obtain

$$G_{j(j+1)}^* = \left[\frac{2\pi\left(R_{(j+1)}^*\right)^3}{S^2\left(1 - a_{(j+1)}^*\right)\left(B - T_{MZ}\right)}\right]\left(\frac{dT}{dR}\right)_{R = R_{(j+1)}^*} , \tag{47}$$

where the term a has been replaced by $a^*_{(j+1)}$, its value at the range $R^*_{(j+1)}$. For the pattern determination, we assign this value of $G^*(\alpha)$ to the midpoint of the interval $(\alpha^*_j, \alpha^*_{(j+1)})$, that is

$$\alpha^*_{j(j+1)} = 1/2\left(\alpha^*_j + \alpha^*_{(j+1)}\right) . \tag{48}$$

With the angle restricted to small values, Equations (42), (43) and (48) may be combined to yield

$$\alpha^*_{j(j+1)} = \frac{S}{4R^*_{(j+1)}}\left(1 + \sqrt{2}\right) . \tag{49}$$

Discrete points $(\alpha^*_{j(j+1)}, G^*_{j(j+1)})$ of the pattern are then obtained from Equations (47) and (49).

Let us now compare these results with those obtained when the reflector was approximated by a circular disk. For this comparison, we refer to Equation (21) from which the earlier results were derived. It will be convenient to derive a new expression for $G_{j(j+1)}$ from this equation. Differentiating with respect to R and evaluating the results for a range $R_{(j+1)}$ yield

$$\left(\frac{dT}{dR}\right)_{R = R_{(j+1)}} = -1/2\left(1 - a_{(j+1)}\right)\left(B - T_{MZ}\right) G_{j(j+1)} \sin \alpha_{(j+1)} \left(\frac{d\alpha}{dR}\right)_{R = R_{(j+1)}} . \tag{50}$$

Referring to Equations (20) and (36) and recalling that α is a small angle, we find that

$$\sin \alpha_{(j+1)} \left(\frac{d\alpha}{dR}\right)_{R = R_{(j+1)}} = -\frac{S^2}{\pi R^3_{(j+1)}} . \tag{51}$$

Combining the last two equations and solving for $G_{j(j+1)}$ yield

$$G_{j(j+1)} = \frac{2\pi R^3_{(j+1)}}{S^2\left(1 - a_{(j+1)}\right)\left(B - T_{MZ}\right)} \left(\frac{dT}{dR}\right)_{R = R_{(j+1)}} . \tag{52}$$

Referring to Equation (13) and (36), we note that the value of α for which Equation (52) applies is well approximated by

$$\alpha = \frac{S}{R_{(j+1)}\sqrt{\pi}} \quad . \tag{53}$$

If Equations (52) and (53) with $R_{(j+1)} = R^{*}_{(j+1)}$ are compared respectively to Equations (47) and (49), it will be observed that the expressions for the effective power pattern of the antenna are identical while the two values of the angle α are in the ratio of

$$\left(\frac{1 + \sqrt{2}}{4}\right) \Big/ \left(\frac{1}{\sqrt{\pi}}\right) = 1.070 \ .$$

This suggests that, in using the results obtained with Equation (24) which is essentially equivalent to Equation (52), the angle $\alpha_{j(j+1)}$ given by Equation (25) is in error by 7 percent and should be corrected by the factor 1.070.

Summary

To summarize, the computing procedure for determining the effective power pattern of an antenna, with appropriate corrections for the approximation of the reflector by a circular disk, consists of the following.

1. For $\alpha \leq \bar{\alpha}$ the parameters $\bar{\alpha}$, b, and B are determined by fitting to the measured data with the method described in Appendix B; G_o is evaluated from Equation (17); and the effective power pattern of the antenna is computed from

$$G(\alpha) = G_o e^{-(3/\pi)b\alpha^2} \quad . \tag{54}$$

2. For $\alpha > \bar{\alpha}$, a sufficient number of discrete points $(\alpha_{j(j+1)}, G_{j(j+1)})$ to characterize the pattern are determined by using Equation (24) to compute $G_{j(j+1)}$ while obtaining a

corrected value of $\alpha_{j(j+1)}$ from the expression

$$\alpha_{j(j+1)} = 0.535\left(\alpha_j + \alpha_{j+1}\right) . \tag{55}$$

SECTION III

ANTENNA PERFORMANCE EVALUATION

In normal operation, performance of a radiometric antenna is judged by its ability to discern a target in front of, or partially behind, a background of vegetation which has a radiometric temperature nearly equal to the ambient temperature. A measure of this performance is the maximum operable range of the antenna for a fixed-size target, or alternatively, the maximum contrast between the background temperature and the measured temperature for a fixed-size target at a given range.

The VARR method offers a relatively simple procedure of measurement and analysis to systematically rate the performance of various antenna systems on the basis of a comparative evaluation. It has been used to establish the characteristics of numerous antenna systems and from these, to evaluate the performance of the antennas on a relative basis. In general, the results obtained by the VARR method agree well with the previously noted effectiveness of these same antennas in field operations. Although some parameters differ substantially from theoretical values, the trends which were established prove to be very useful in comparing the performance of the various systems.

Results are presented for a total of eight different antennas. Tabulations of antenna type, frequency, and several theoretical parameters are given in Table I. Identification is provided by the tabulated run number. The term ρ is defined to be the range from the antenna to the closest portion of the far-field. It is computed from

$$\rho = 2D^2/\lambda \ , \tag{56}$$

where D is the diameter of the antenna aperture and λ is the wavelength. The theoretical gain G_t amd theoretical 3 db beamwidth θ_t are calculated values which were obtained from the following equations:

$$G_t = 0.5\left(\frac{\pi D}{\lambda}\right)^2 \ , \tag{57}$$

$$\theta_t = 1.2(\lambda/D) \ . \tag{58}$$

TABLE I.

ANTENNA TYPE AND THEORETICAL PARAMETERS

Run Number	Antenna Type	Freq., Gc	λ, ft	ρ, yds	θ_t, deg	G_t, db
1	18" Plano Convex Lens	68.5	0.0144	104	0.66	47.3
2	36" Parabola	68.5	0.0144	417	0.33	53.3
3	18" Plano Convex Lens	140	0.0070	214	0.32	53.6
4	18" Fresnel Zone Plate	140	0.0070	214	0.32	53.6
5	36" Cassegrainian	35	0.0281	214	0.64	47.5
6	18" Plano Convex Lens	94	0.0105	143	0.48	50.0
7	36" Scalar Feed Parabola	94	0.0105	571	0.24	56.1
8	36" Circular Scan Parabola	68.5	0.0144	417	0.33	53.3

TABLE II.

MEASURED DATA AND COMPUTED PARAMETERS

Run No.	T_{MZ}, ^oK	T_{MB}, ^oK	Absolute Hum., g/m^3	Computed 3db Beamwidth, deg	Computed 20 db Beamwidth, deg	Ratio of 20 db to 3 db Beamwidth	Temperature contrast at R = 800 yds, ^oK	Computed Gain, db
1	93	256	5.1	0.65	3.4	5.2	14	46.8
2	120	266	10.2	0.76	4.2	5.5	11	45.4
3	112	289	9.0	0.64	2.8	4.4	18	47.8
4	135	287	13.4	0.68	3.4	5.0	15	46.6
5	30	273	9.1	0.73	2.0	2.7	25	47.5
6	94	253	5.1	0.64	2.4	3.7	30	48.2
7	47	209	1.9	0.60	1.4	2.3	29	50.4
8	135	275	9.8	0.67	4.0	6.0	8	45.8

An antenna efficiency of 50 percent was assumed in computing the theoretical gain. Table II presents a tabulation of some of the measured quantities and a number of the more significant parameters arising from the analysis of the observed data. Both the gains and the beamwidths in Table II were derived from the VARR data. The entire set of measurements, together with the resulting patterns, are plotted in Figures 5 through 20. These figures have been arranged to present the measurements and resulting patterns of each run side by side. The measurements for most runs were repeated at least once and it was found that corresponding observations generally agreed to within one degree Kelvin, which was the measuring accuracy of the instrumentation system.

At the 3 db points, the patterns obtained by the VARR method are usually wider than the theoretically computed beamwidths. Also, the measured antenna gains, while still useful for a comparative evaluation of the antennas, are generally several db less than the theoretical values. The smaller gains are, of course, consistent with the wider beamwidths. While some beam broadening and loss of antenna gain are to be expected from inaccuracies in field measurements and atmospheric effects which may not have been properly taken into account, it is believed that the primary source of difficulty arises from the non-coherent nature of the signals. Consider the two plots of temperature versus range presented in Figure 21. The upper curve is simply a plot of the VARR observations for Run No. 7, whereas the other curve was computed for an antenna having the theoretical gain and beamwidth given for the "Scalar Feed" antenna used in obtaining the data shown in Table I. The background and zenith temperatures were assumed to be identical to the measured values for Run No. 7. The huge discrepancy between the actual measurements and the theoretical curve cannot be explained satisfactorily by attenuation effects or, for that matter, any other likely source of error. A plausible explanation appears to be that the broader beamwidth does, indeed, result from the non-coherent nature of the signals. This effect has also been reported by Fedoseev[1].

---

[1] *Fedoseev, L. I. "Lunar and Solar Radio Emission at 1.3 mm Wavelength". Radiofisika, Volume VI, Number 4: 655-659, 1963*

Referring to Table II, it will be observed that certain antennas show a definite superiority in all comparisons. Of particular significance are the beamwidths at the 3 db and the 20 db points on the measured patterns where the comparisons reveal a pronounced difference between certain antennas. In all cases, the antennas which had wider 20 db beamwidths also had poorer operating performance and showed much less contrast between measured and background temperatures with the reflector at a range of 800 yards. The ratio of the 20 db beamwidth to the 3 db beamwidth is tabulated in Table II. This ratio is a good indication of the relative merit of antennnas that have different apertures and operate at different frequencies. In general, the plano-convex lens antennas were among the better performers while the TRG corporation "Scalar Feed" type was the best.

In comparing the results for these various antenna systems, a number of additional factors should be considered. One of these which may have contributed to the low performance of the poorer antennas was the critical adjustment necessary for focusing. The feed horn positions on the conical scan and the parabolas were very critical while the lens antenna feeds were quite easy to position, maintaining relatively equal performance over a relatively wide range of adjustment. The "scalar Feed" antenna, while also very critical to adjust, was built more solidly and could maintain its adjustment while handled in the field. The Fresnel zone-plate, another poor performer, had high side lobes probably due to reflections at the discontinuities caused by the zone cuttings. The Cassegrainian, also a critical antenna to adjust, performed reasonably well, but was not as efficient as the "Scalar Feed". One of the factors affecting system performance while using a particular antenna is not included in this evaluation. This factor is the loss peculiar to an antenna type. In general, the shepherd's crook feed has considerable wave-guide loss; but on the other hand, the lens antenna suffers a loss in the dielectric of the lens itself. The Cassegrainian feed probably has the least loss due to the feed system, but it also may have increased spillover from the double reflecting system.

An exhaustive error analysis of the reported results has not been attempted; but this phase of the problem has been treated in sufficient detail to conclude that the accuracy of the method is, in fact, somewhat better than originally anticipated. Error estimates have been computed for the central portion of the pattern on the basis of the least squares fit. For the eight runs reported upon, the average probable error in antenna gain was 0.2 db and in background temperature, 1.7°. In general, the probable error in the central portion of the pattern was found to be well under 5 percent of the antenna gain while, for the remainder of the pattern, it rarely exceeded 5 percent. The primary sources of error have been considered in detail elsewhere in this report and the discussion will not be repeated. However, it should be emphasized that the errors introduced by including observations with the reflector in the near-field do not greatly reduce the usefulness of the results. Those portions of the patterns drawn as solid lines are entirely free of such error. Moreover, the dashed curves immediately adjacent to the solid curves are relatively free of this type of error since it enters very gradually as the range of the reflector decreases from the transition value of $2D^2/\lambda$. An examination of the plotted results reveals that the essential characteristics of the antenna patterns are generally well determined in spite of a slight distortion in the sides of the patterns as a result of the inclusion of observations with the reflector in the near-field.

CONCLUSION

The VARR method offers a practical and relatively simple approach for the comparative evaluation of radiometric antenna systems. The effort involved is a fraction of that required to achieve equivalent results by conventional methods. In addition, the effective power pattern and gain characteristics are determined by the VARR technique with the antenna in an operational environment. The measurements are made under field conditions similar to those to be expected in proposed applications of the antenna systems. Hence, the method provides a simple means of pattern determination, and perhaps, offers a more accurate evaluation of antenna performance under realistic operating conditions.

While the derivation of the VARR computing procedure is somewhat involved, its application is straight forward, routine, and comparatively simple. The method has been programmed for computation on a high speed digital computer, but it is not unrealistic to perform all the necessary computations on a desk calculator or even a slide rule. The computing time required per run is less than one minute on a high speed machine in contrast to an hour and a half on a desk calculator.

Effective power patterns have been determined successfully for a number of antennas by this technique. In general a comparative evaluation of the VARR results agreed well with the observed effectiveness of the same antenna in earlier measurements. An error analysis of the results indicated the method to be somewhat more accurate than expected. On the other hand, the computed power patterns reveal a broader beam than coherently measured patterns for the same antennas; but it appears that the beam broadening may well have resulted from the non-coherent nature of the signals. In any event, the effective power patterns obtained by the VARR method provide a reliable basis for predicting the relative radiometric performance of antenna systems in an operational environment.

R. B. PATTON C. L. WILSON

BIBLIOGRAPHY

1. Bauerle, D. G., Wilson, C. L., and Richer, K. A. Millimetric Wave Research For Guidance Application. Proc. Electromagnetic Warfare Symp. on MM. Wave Tech. Johns Hopkins University, November 1963. (SECRET)

2. Baurele, D. G. Ground Radiometric Measurements at 2.17 Millimeters. (U) Ballistic Research Laboratories Memorandum Report No. 1658, June 1965. (CONFIDENTIAL)

3. Blake, Lamont V. Low-Noise Receiving Antennas. Microwaves, 18-27 March 1966.

4. Bolgiano, L. P. General Considerations Governing the Possible Use of Microwave Techniques for Missile Guidance. (U) Ballistic Research Laboratories Report No. 1166, April 1962. (CONFIDENTIAL)

5. Hornak, D. L., and Wilt, R. E. Millimeter Wave Radiometer Program. (U) (Ballistic Research Laboratories Contract DA 01-009-AMC-1085X). Sperry Microwave Electronics Co., Report S. J. 212-0042-14 C-5495A-1, December 1963. (CONFIDENTIAL)

6. Kay, Alan F. The Relationship of Antenna Performance and Contrast Temperatures in Radiometers With Application to Ground Targets In The Near and Far Fields. (Ballistic Research Laboratories P.O. 1095). TRG No. S-302, March 1965.

7. Lamphears, H. F., and Wilt, R. E. Radiometric Temperature Measurement Program. (U) (Ballistic Research Laboratories Contract DA 01-009-AMC-69R). Sperry Microwave Electronics Company: Ref A02195, December 1963. (CONFIDENTIAL)

8. Richer, K. A., and Baurele, D. G. Near-Earth Millimeter Wave Radiometer Measurements. Ballistic Research Laboratories Report No. 1267, December 1964.

9. Richer, K. A., and Kammerer, J. E. 70 Gc Radar Characteristics Measurement for American and Russian Targets. (U) Ballistic Research Laboratories Memorandum Report No. 1683, June 1965. (CONFIDENTIAL)

10. Roberts, J. Radiometric Pointing Errors and Target Isotherms. (U) Ballistic Research Laboratories Memorandum Report No. 1667, June 1965. (CONFIDENTIAL)

11. Rosenthal, Myron, Biagi, Fred, and Lewinter, Sidney. Final Report on a Millimeter Wave Radiometer Guidance Measurement Program. (U) (Ballistic Research Laboratories Contract DA-30-064-AMC-621(R)). General Precision, Inc,: GPI K20910, October 1964. (CONFIDENTIAL)

12. Seelig, S. M. Final Technical Report on Radiometric Signatures of Battlefield Targets. (U) (Ballistic Research Laboratories Contract DA-30-069-ORD-3507). General Precision, Inc.: GPL Sec. P0429-A, April 1962. (CONFIDENTIAL).

13. Silver, Samuel, Microwave Antenna Theory And Design. New York: McGraw-Hill Book Company, Inc., 1949.

14. Strum, Peter D. Considerations in High-Sensitivity Microwave Radiometry. Proc. IRE, 46, 43-53: January 1958.

15. Wentworth, F. L. High Sensitivity Millimeter Wave Receiver. (Ballistic Research Laboratories Contract DA-36-034-ORD-3509RD). Electronics Communications, Inc.: ECI R 62-45: FR-70, November 1962.

APPENDIX A

THE EFFECT OF A NONHOMOGENEOUS BACKGROUND TEMPERATURE SOURCE

Background temperature for antenna pattern determination has normally been measured with the antenna axis directed horizontally toward a background of trees and with the reflector entirely removed from the field of view of the antenna. In general, it has been assumed that this temperature is invariant with direction whereas it varies considerably with elevation for frequencies below 68.5 Gc. The measured background temperature is, in fact, an average radiometric temperature which results from the combined radiation of the atmosphere in the direction of the background vegetation, the atmosphere in the direction of the sky, and the background vegetation itself. It has been shown in the main body of the report that the assumption of a constant background temperature is a reasonable approximation for narrow beam antennas operating at frequencies of 68.5 Gc and higher. The effect of such an assumption for lower frequencies will now be considered.

We will assume that the background consists of trees, whose height above the level of the antenna is h, and of course, sky above the trees. For simplicity in the analysis, it will be assumed that the background as viewed from the antenna radiates at a temperature T_B for heights not exceeding h and a variable temperature $T(\varepsilon)$ for heights in excess of h where ε is an elevation angle measured from the antenna site. Moreover, we will limit our discussion to the case where the reflector is assumed to be a circular disk.

Recalling that α is one-half the angle subtended by the reflector, consider the case where

$$\alpha < \tan^{-1}(h/R_B) \ . \tag{A1}$$

R_B is defined to be the horizontal range from the antenna to the background of trees. To simplify the discussion, power losses in the atmosphere and rf system will be neglected. With these assumptions and the aid of

Figure 22, we may express the measured temperature as

$$T_M(\alpha) = \frac{1}{4\pi}\left[T_Z \int_0^{2\pi}\int_0^{\alpha} G(\theta)\sin\theta\, d\theta\, d\phi + \int_0^{\pi}\int_{\eta}^{\frac{\pi}{2}} T(\varepsilon)G(\theta)\sin\theta\, d\theta\, d\phi\right.$$

$$\left. + T_B\left\{\int_0^{\pi} I_{\alpha}^{\eta}\, d\phi + \int_{\pi}^{2\pi} I_{\alpha}^{\frac{\pi}{2}}\, d\phi\right\}\right], \tag{A2}$$

where

$$\eta = \tan^{-1}(h \csc\phi/R_B). \tag{A3}$$

Equation (A2) may be more conveniently written as

$$T_M(\alpha) = T_B - 1/2(T_B - T_Z)I_o^{\alpha} - \tag{A4}$$

$$1/4\pi \int_0^{\pi}\int_{\eta}^{\pi/2}\left\{T_B - T(\varepsilon)\right\}G(\theta)\sin\theta\, d\theta\, d\phi$$

where

$$\varepsilon = \sin^{-1}(\sin\theta\sin\phi). \tag{A5}$$

If the Equation (A4) is compared to Equation (12) with a = 0, it is apparent that the error resulting solely from the nonhomogeneous background temperature consists of

$$\Delta T_M = -\frac{1}{4\pi}\int_0^{\pi}\int_{\eta}^{\frac{\pi}{2}}\left\{T_B - T(\varepsilon)\right\}G(\theta)\sin\theta\, d\theta\, d\phi. \tag{A6}$$

As long as the condition expressed by the inequality (A1) is satisfied, $\eta \leq \alpha$ so that Equation (A2) is valid and ΔT_M remains constant for changes in the parameter α. Therefore, since our methods for evaluating are predicated on the assumption that $G(\alpha)$ is proportional to the derivative of $T_M(\alpha)$ with respect to α, the constant error ΔT_M has no effect on the evaluation of this function.

In considering the measurements reported upon, we are primarily concerned with the effect of the nonhomogeneous background temperature on measurements at the lowest frequency, i.e., 35 Gc. Recognizing this possible source of error, the system geometry for these measurements was designed to satisfy inequality (A1) for all values of α equal to or less than 1.7°. Hence, with narrow beam antennas, the major portion of the effective power pattern determination was free of any error resulting from the nonhomogeneous background source.

APPENDIX B

THE CURVE FITTING PROCEDURE

The computing methods which have been developed for the determination of the central portion of the antenna pattern require a set of observations to be fitted to an exponential curve. In particular, the form of the curve is given by

$$T(\alpha) = Be^{-b\alpha^2}, \tag{B1}$$

for α in the interval $(o, \bar{\alpha})$. The terms $\bar{\alpha}$, b, and B are parameters which are to be evaluated by the fitting procedure.

Let the temperature observations be denoted by T_i and the corresponding values of range by the terms R_i where i constitutes an index for the measured quantities. The observations T_i are paired with the terms α_i where the latter are computed by means of Equation (13) for each range R_i. We observe that Equation (B1) may be written in the form

$$\ln B - b\alpha^2 = \ln T(\alpha). \tag{B2}$$

This suggests that the appropriate range of α for applying the curve fitting procedure may be determined by plotting the points $(\alpha_i^2, \ln T_i)$. Since Equation (B2) is linear in the terms ln T and α^2, $\bar{\alpha}$ may be established to be the largest value of α whereby the plotted points $(\alpha_i^2, \ln T_i)$ lie on a straight line for $\alpha_i \leq \bar{\alpha}$. Let the preceding inequality hold for $i = 0, 1, 2, \ldots, n$.

A least-squares approach has been adopted for the curve fitting procedure. Strictly speaking, the fitting should be applied to B and b in the non-linear Equation (B1). However, the results are sufficiently accurate when we fit for b and ln B by Equation (B2) where these two parameters are linearly related. We define the following matrices:

$$C \equiv \begin{pmatrix} 1 & 0 \\ 1 & -\alpha_1^2 \\ 1 & -\alpha_2^2 \\ \cdot & \cdot \\ \cdot & \cdot \\ \cdot & \cdot \\ 1 & -\alpha_n^2 \end{pmatrix},$$

$$V \equiv \begin{pmatrix} \ln T_o \\ \ln T_1 \\ \ln T_2 \\ \cdot \\ \cdot \\ \cdot \\ \ln T_n \end{pmatrix},$$

$$X \equiv \begin{pmatrix} \ln B \\ b \end{pmatrix}.$$

We note that T_o is, in reality, the measured background temperature; and since this observation applied for $\alpha = 0$, it is included in the curve fitting procedure. Its chief contribution to the computation is to greatly strengthen the determination of the fitted background temperature B. In matrix form, the equations of condition consist of

$$CX = V. \tag{B3}$$

The normal equations are given by

$$C'CX = C'V. \tag{B4}$$

where C' is defined to be the transpose of the matrix C. The least-squares solution is then expressed by the matrix equation

$$X = (C'C)^{-1}C'V, \tag{B5}$$

from which the terms b and ln B, hence B, may be evaluated.

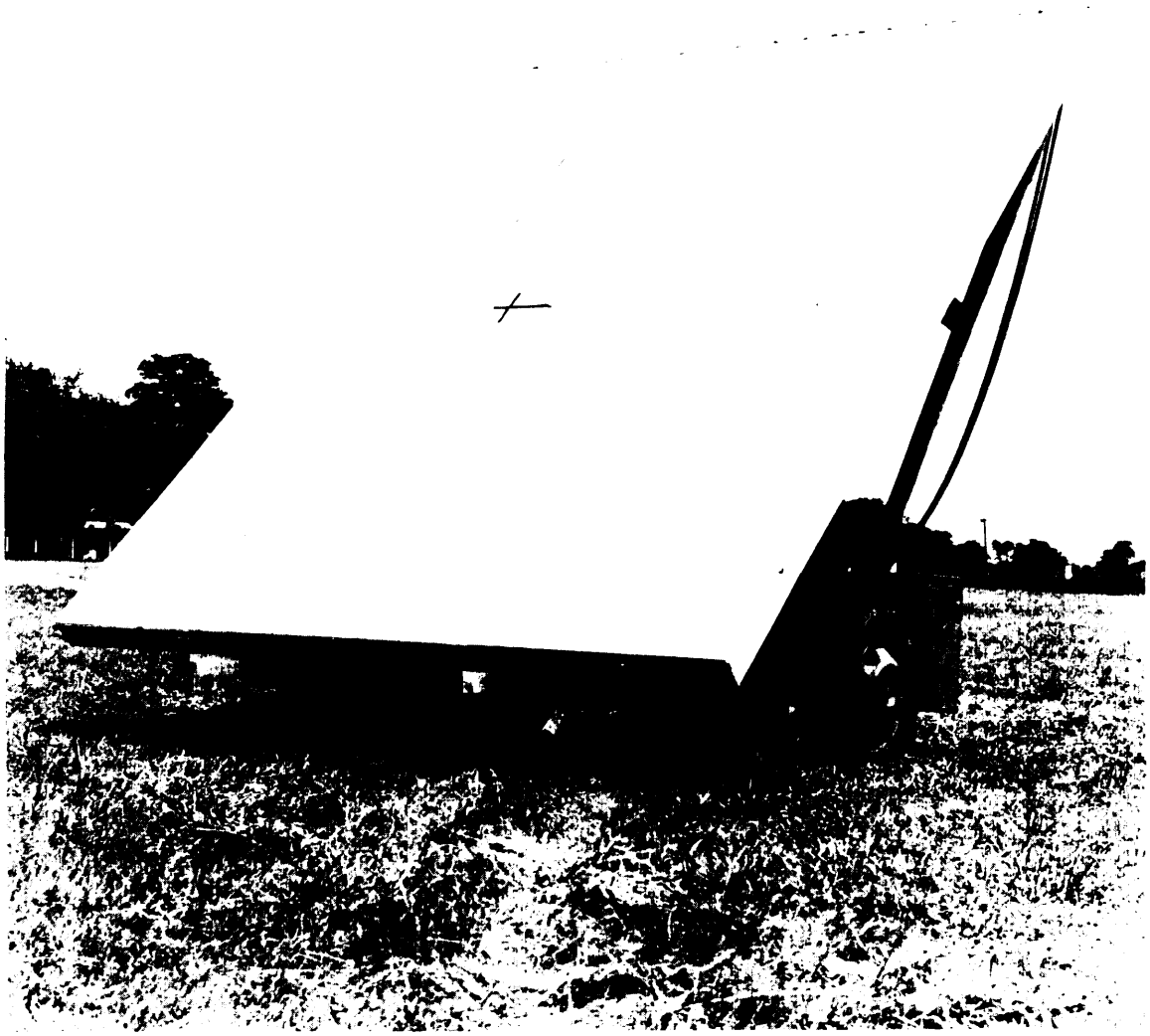

FIGURE 1. THE REFLECTOR

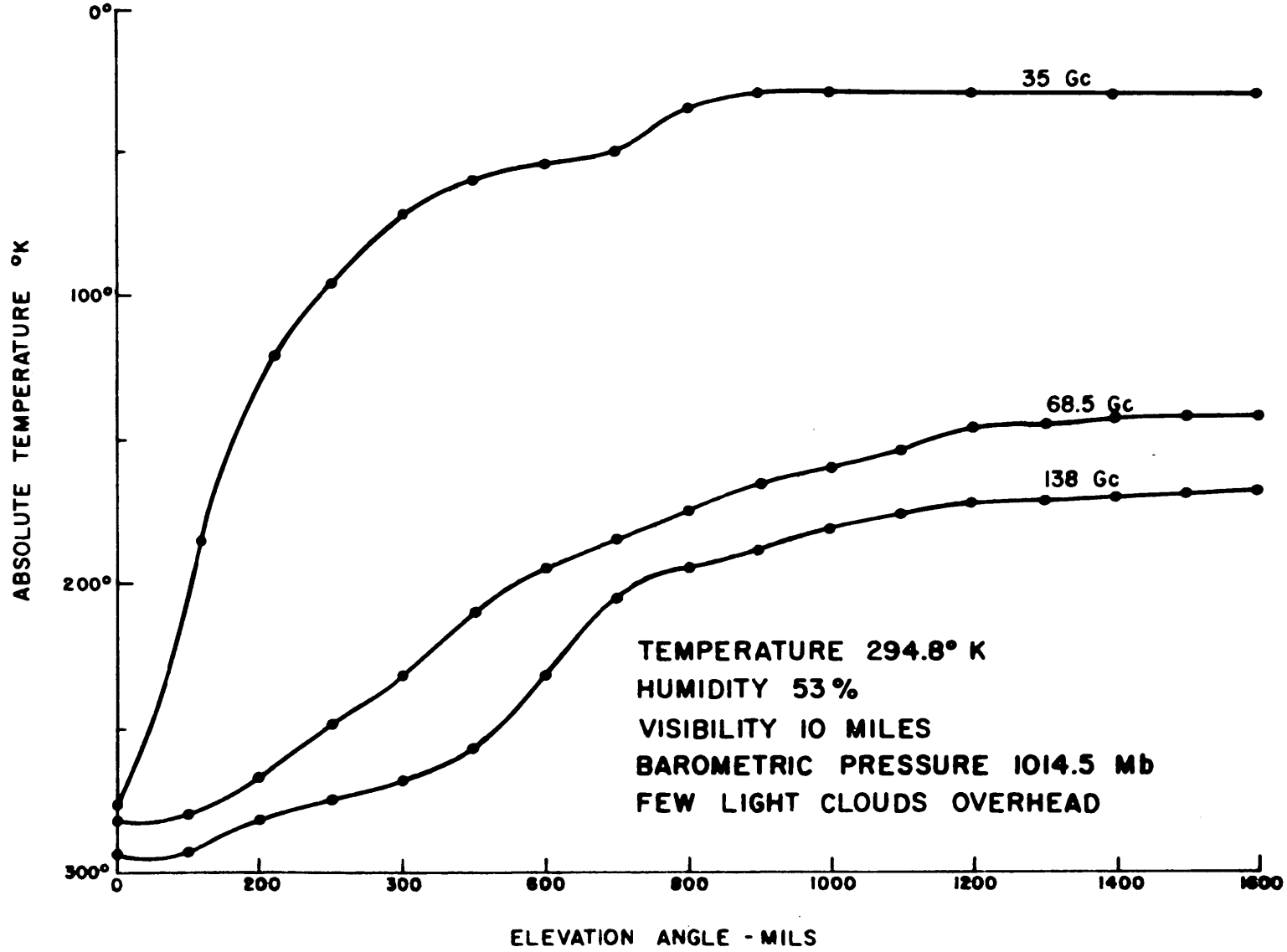

FIGURE 2. RADIOMETRIC TEMPERATURE AS A FUNCTION OF ELEVATION ANGLE AND FREQUENCY

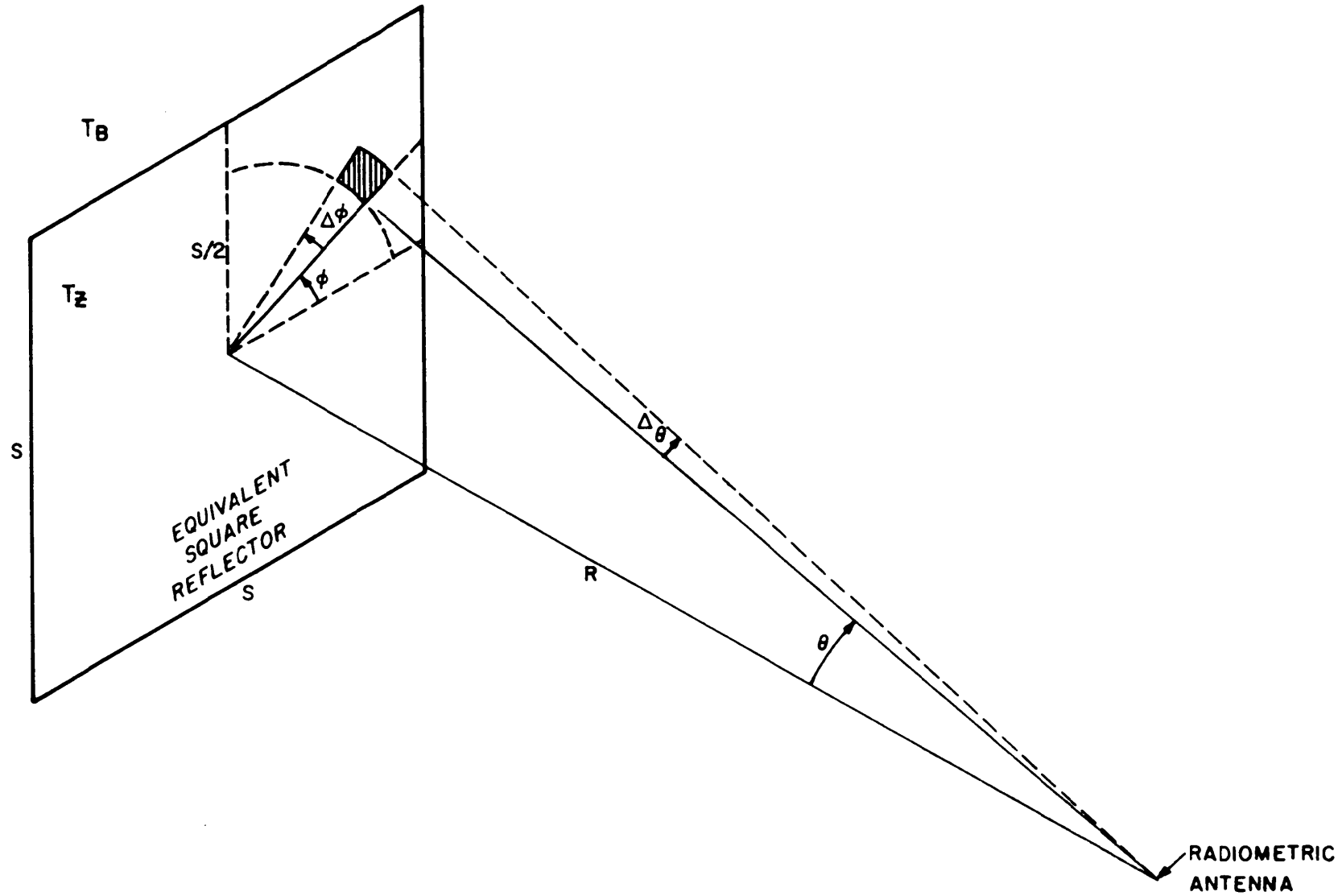

FIGURE 3. VARR SYSTEM GEOMETRY FOR CENTER OF BEAM (SQUARE REFLECTOR)

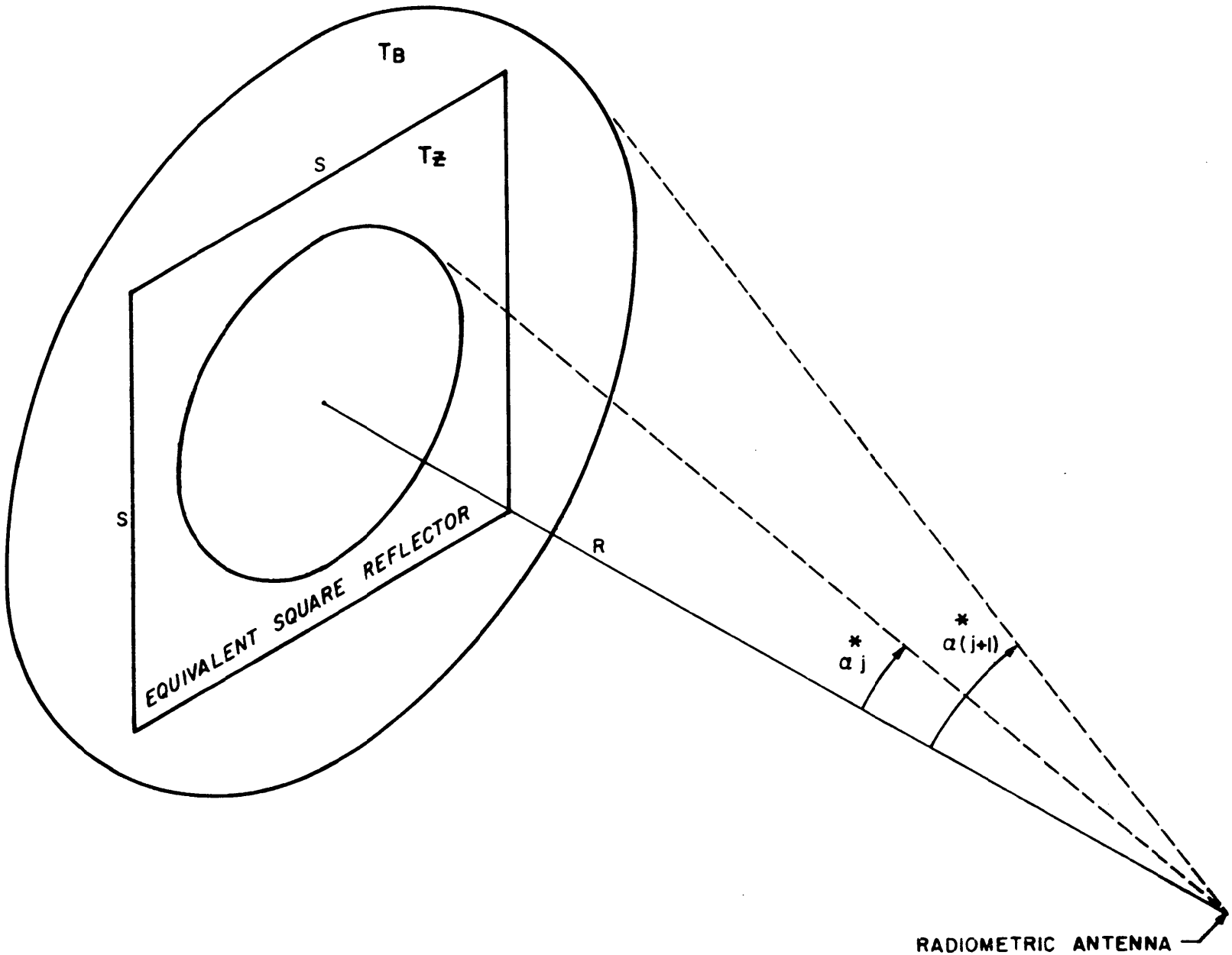

FIGURE 4. VARR SYSTEM GEOMETRY FOR SIDES OF BEAM (SQUARE REFLECTOR)

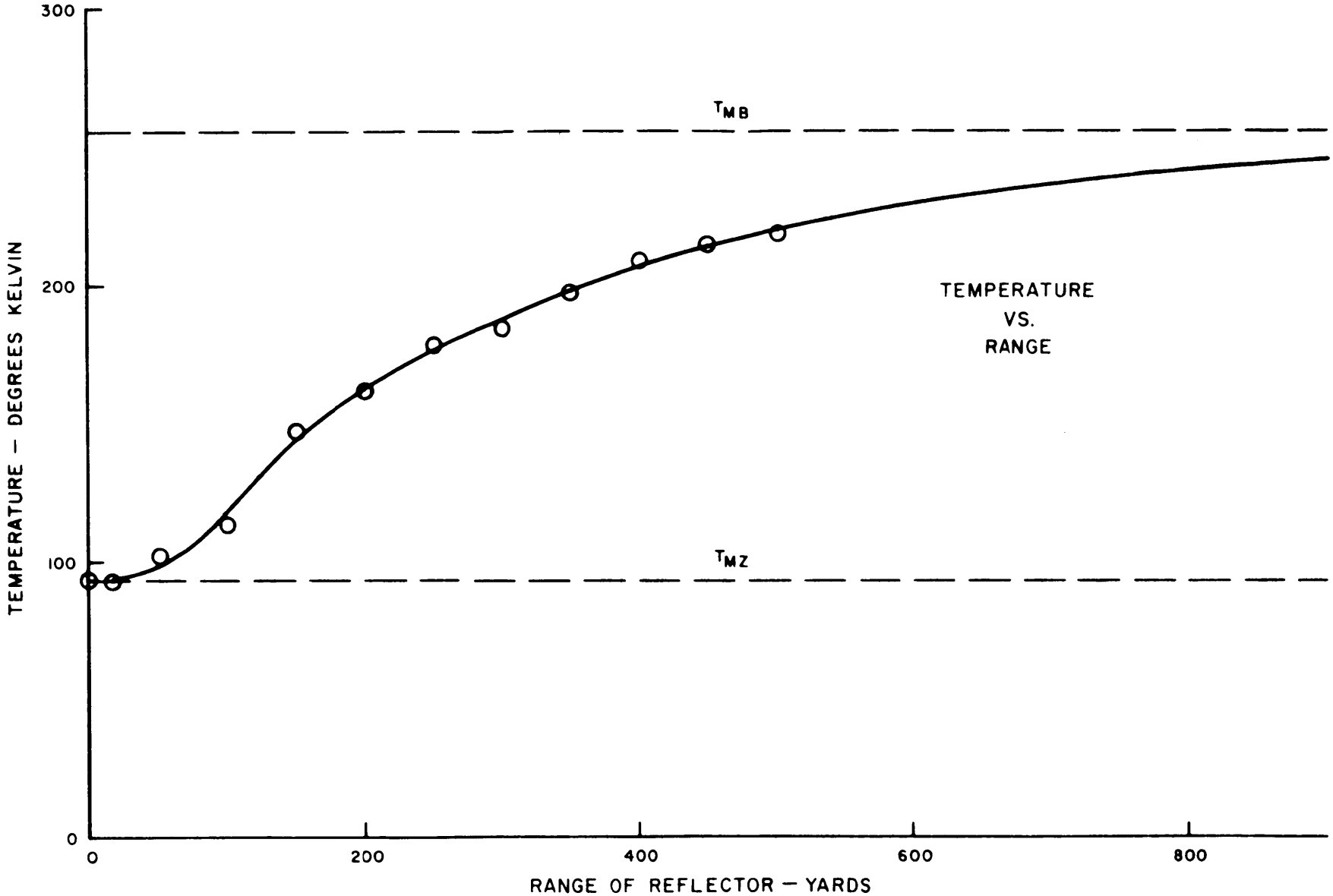

FIGURE 5. MEASURED DATA FOR RUN I.

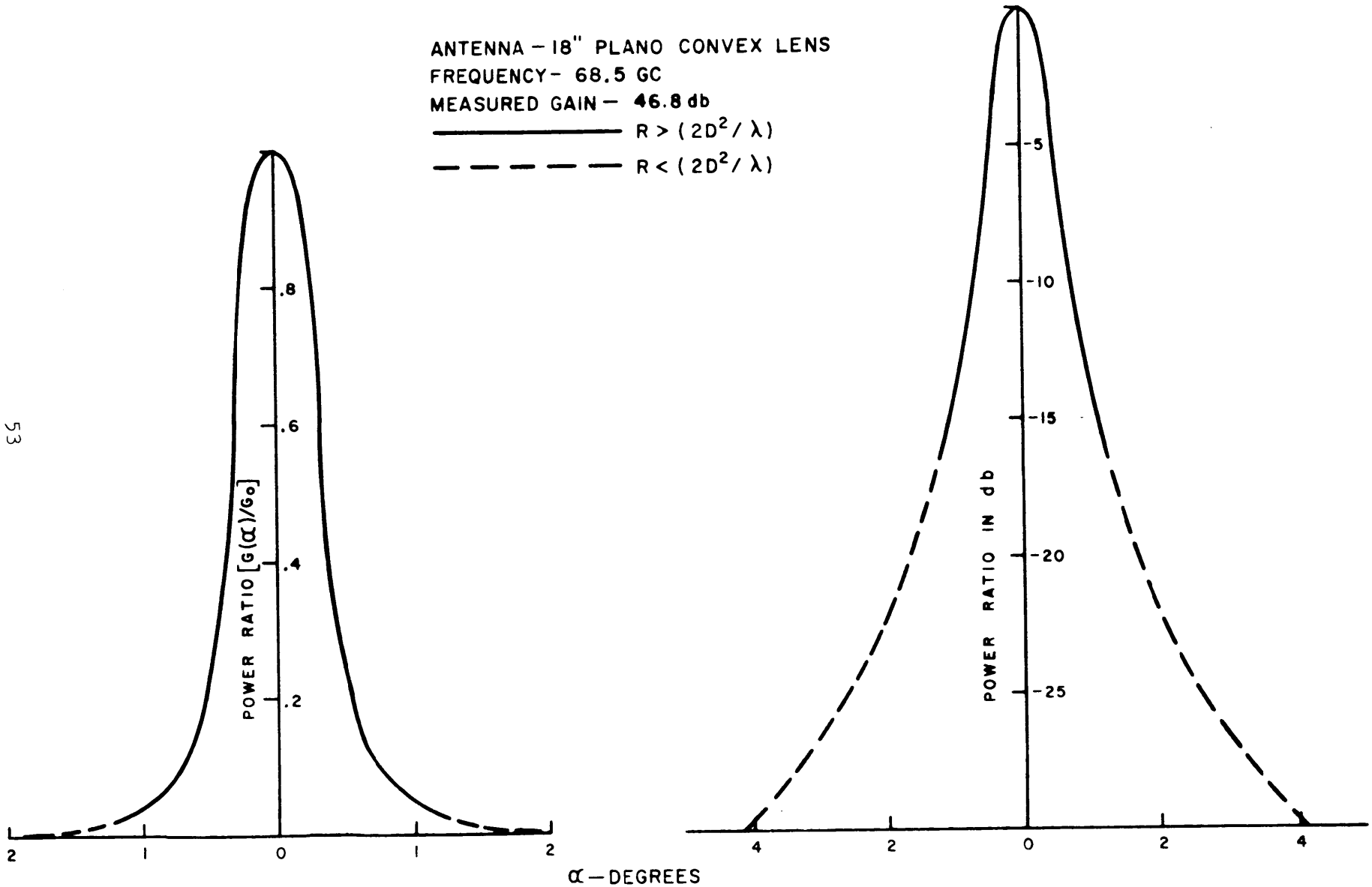

FIGURE 6. NORMALIZED EFFECTIVE POWER PATTERN FOR RUN I.

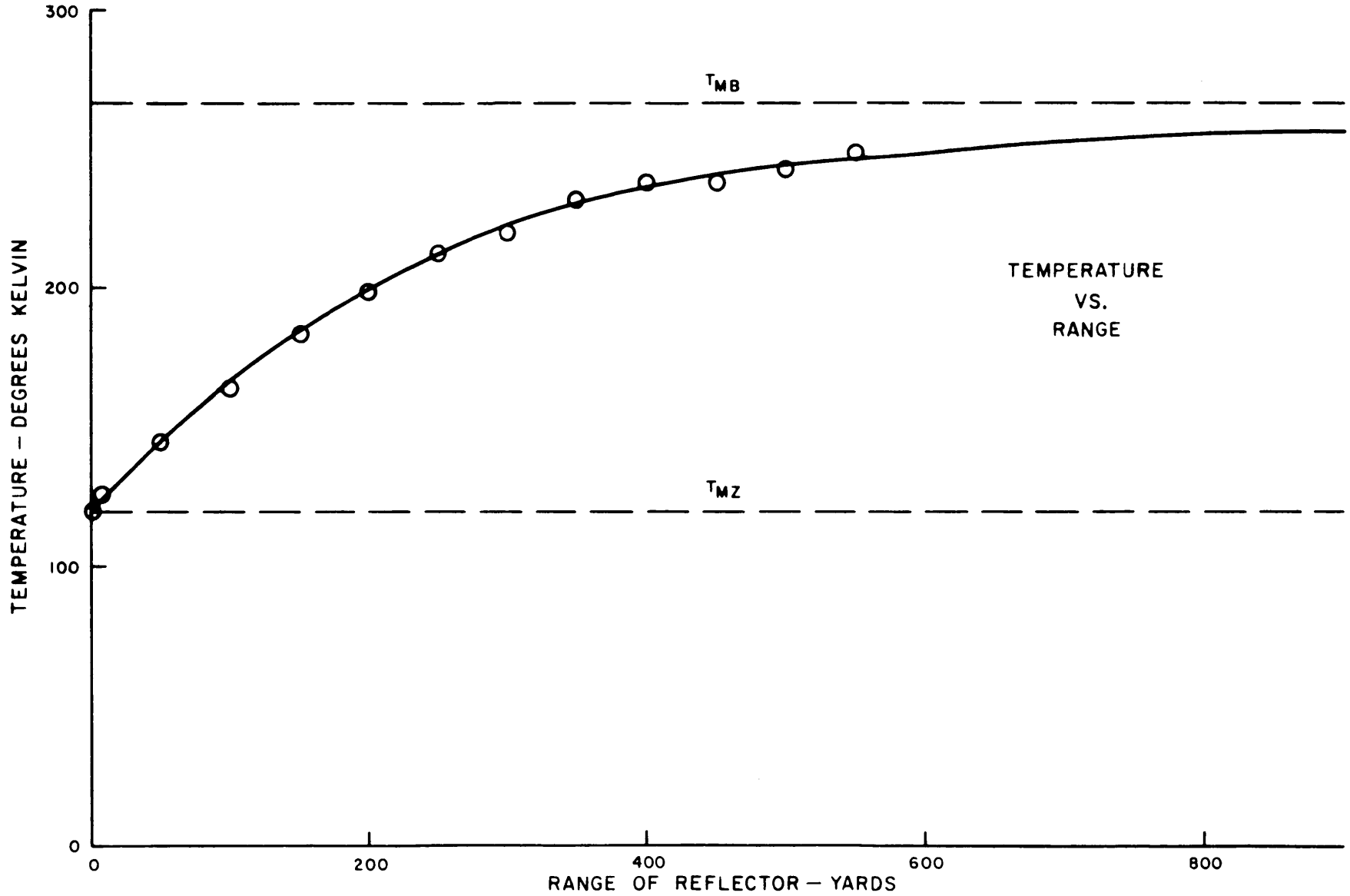

FIGURE 7. MEASURED DATA FOR RUN 2.

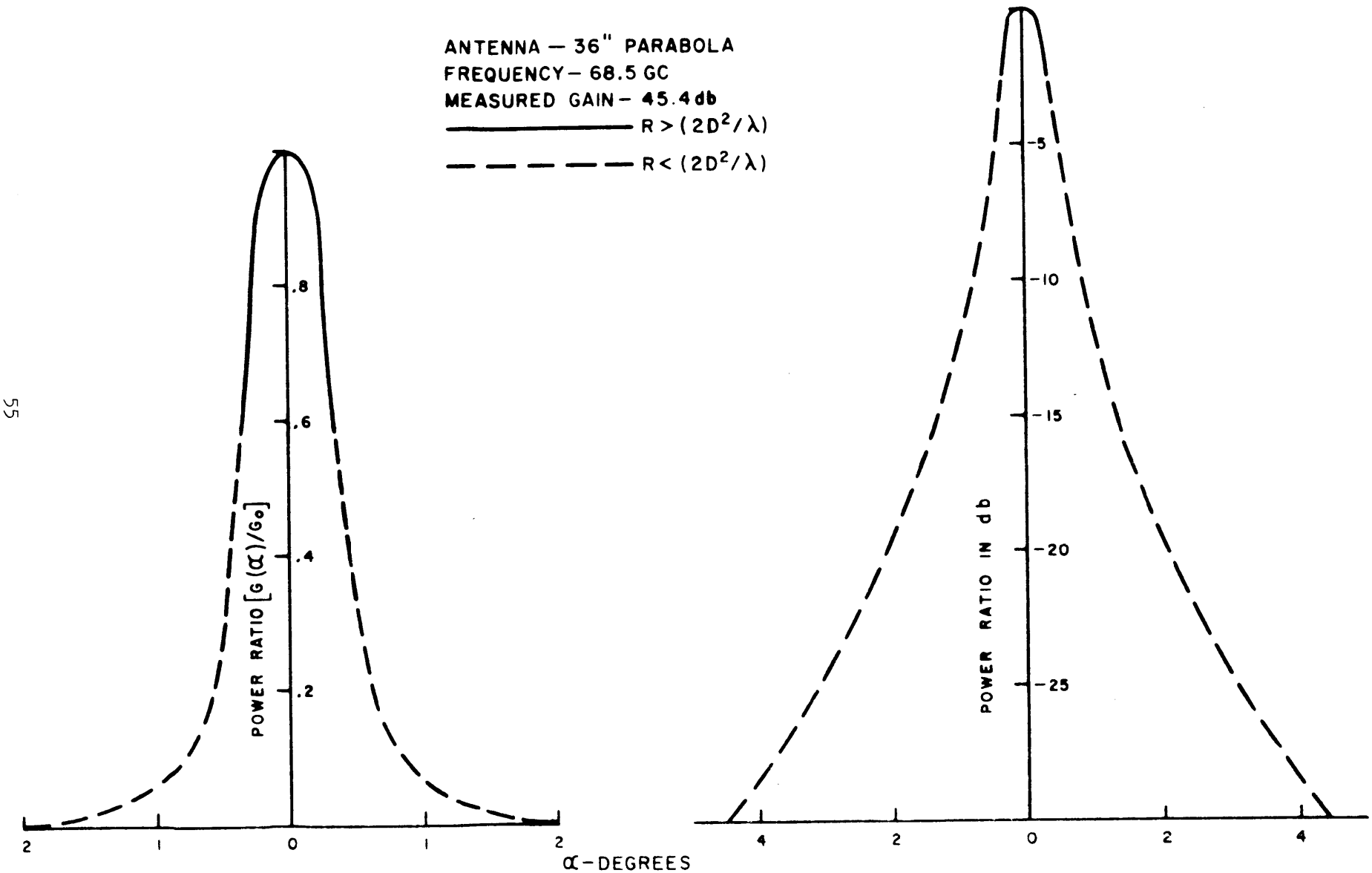

FIGURE 8. NORMALIZED EFFECTIVE POWER PATTERN FOR RUN 2.

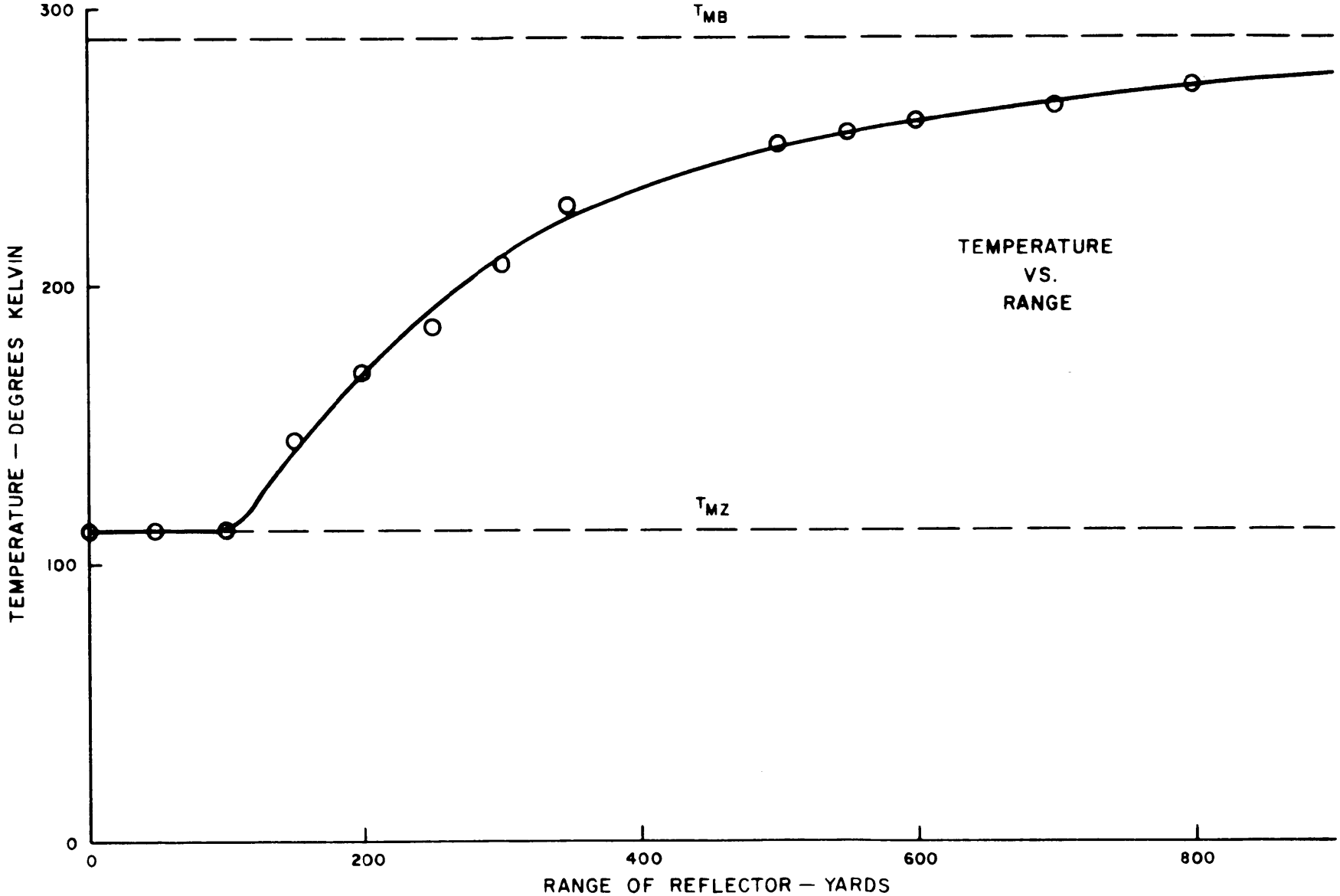

FIGURE 9. MEASURED DATA FOR RUN 3.

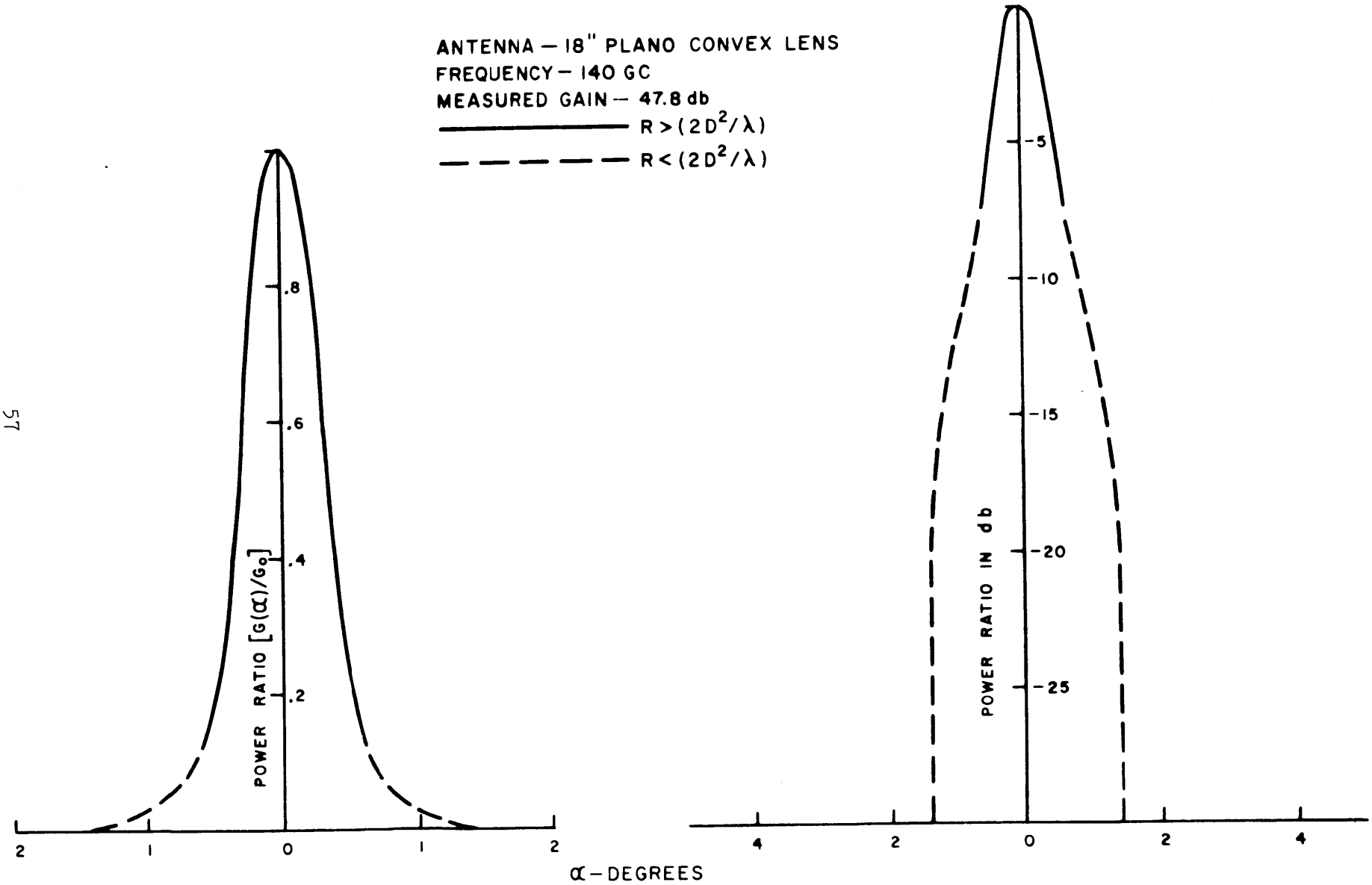

FIGURE 10. NORMALIZED EFFECTIVE POWER PATTERN FOR RUN 3.

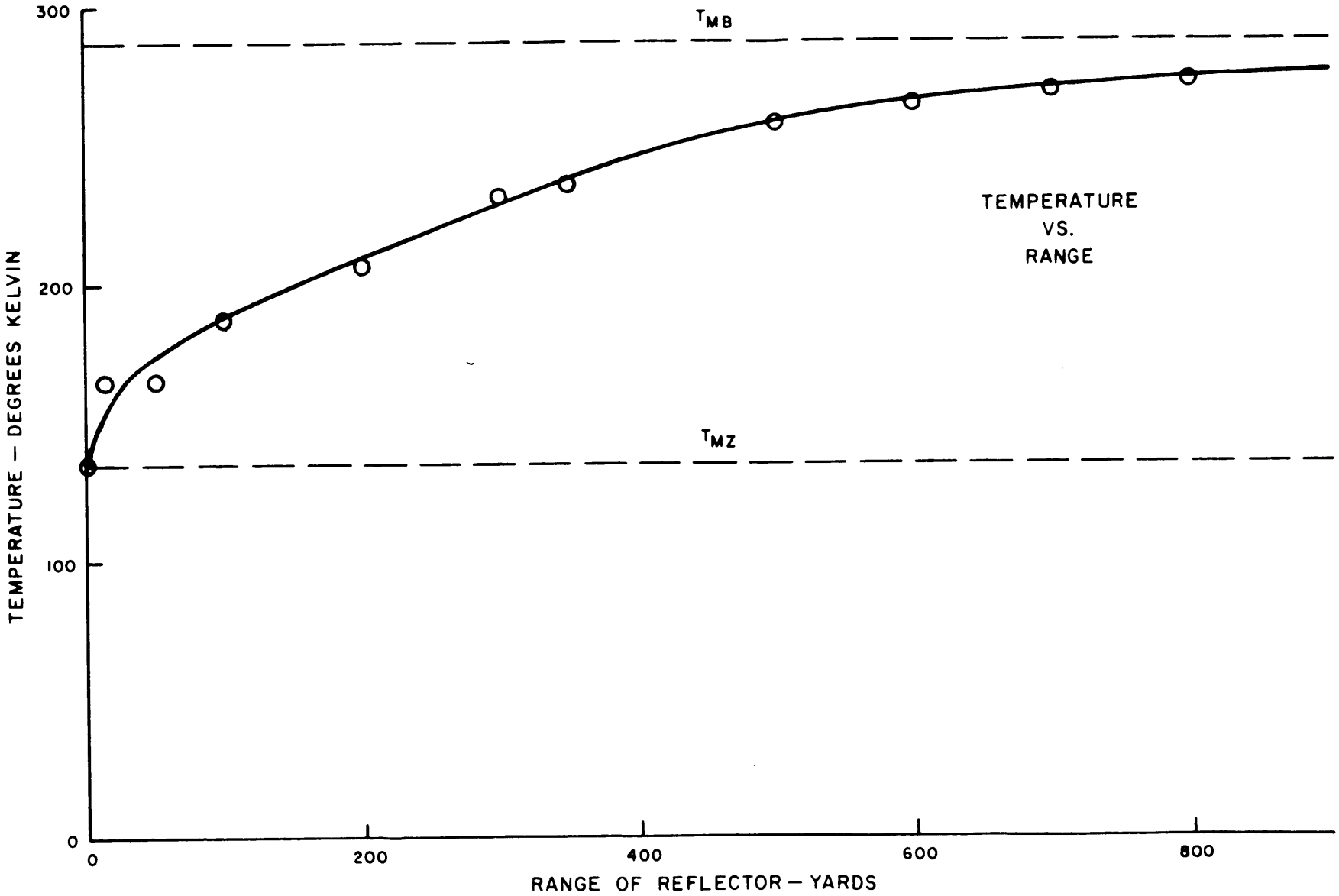

FIGURE 11. MEASURED DATA FOR RUN 4.

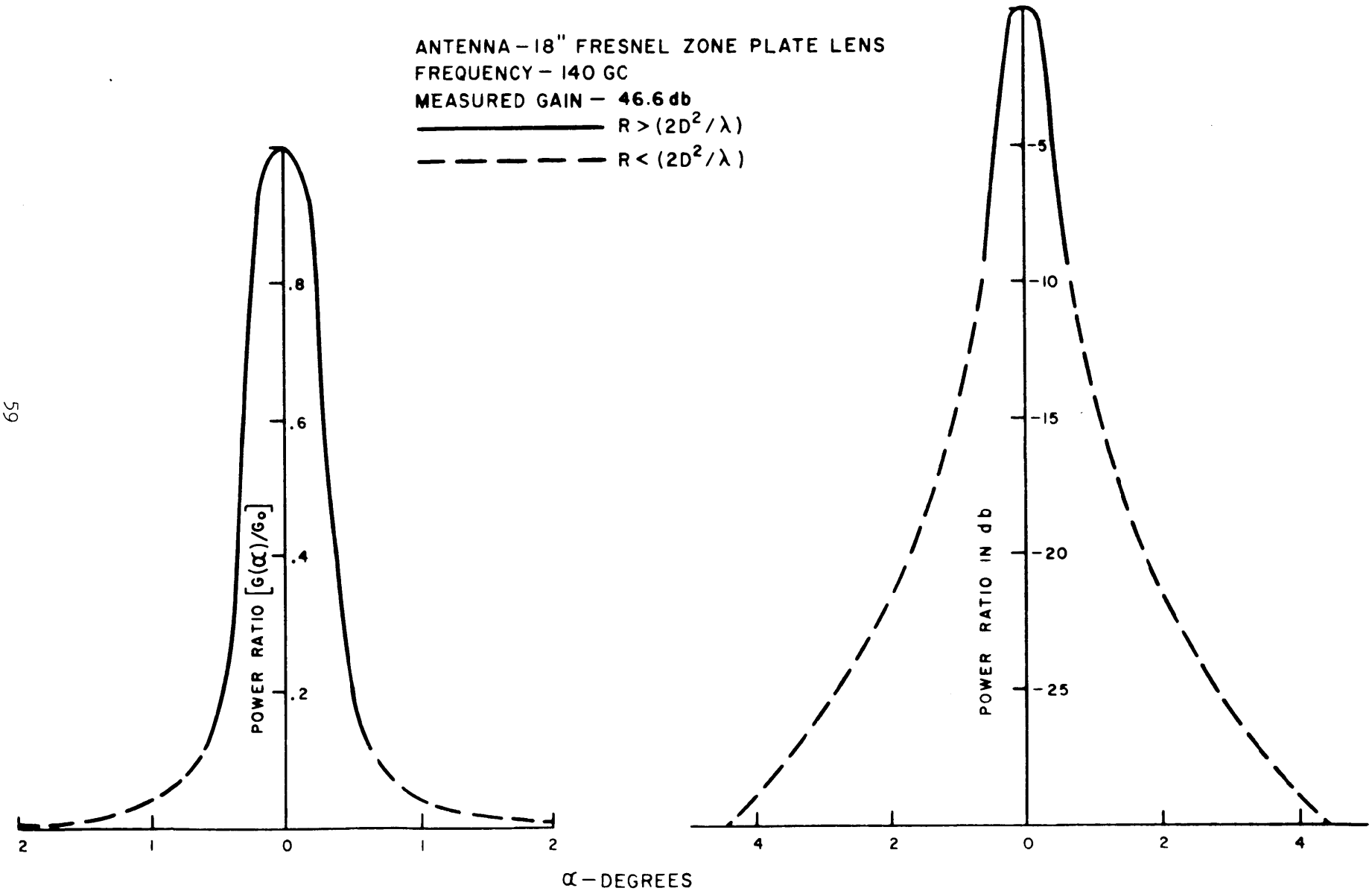

FIGURE 12. NORMALIZED EFFECTIVE POWER PATTERN FOR RUN 4.

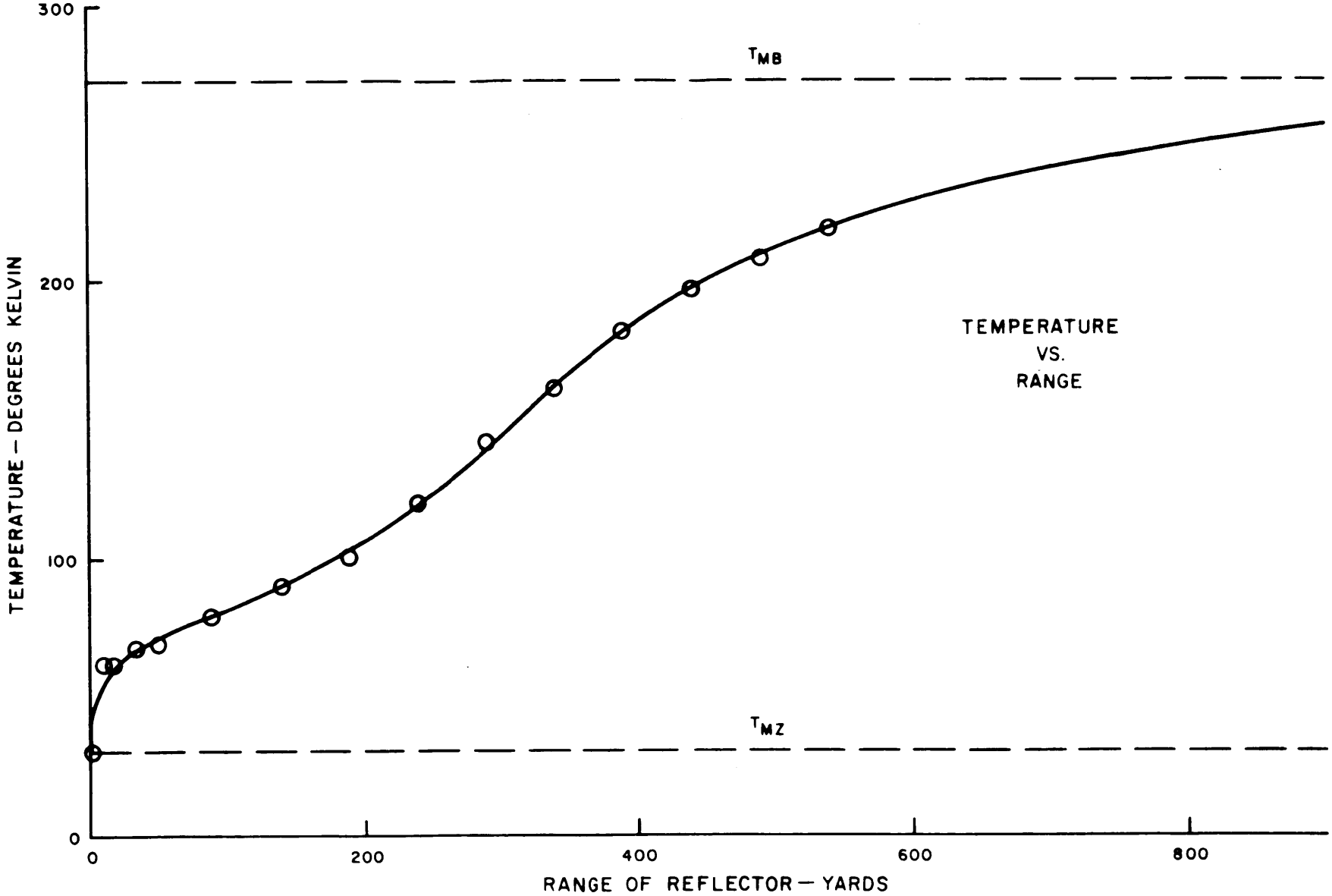

FIGURE 13. MEASURED DATA FOR RUN 5.

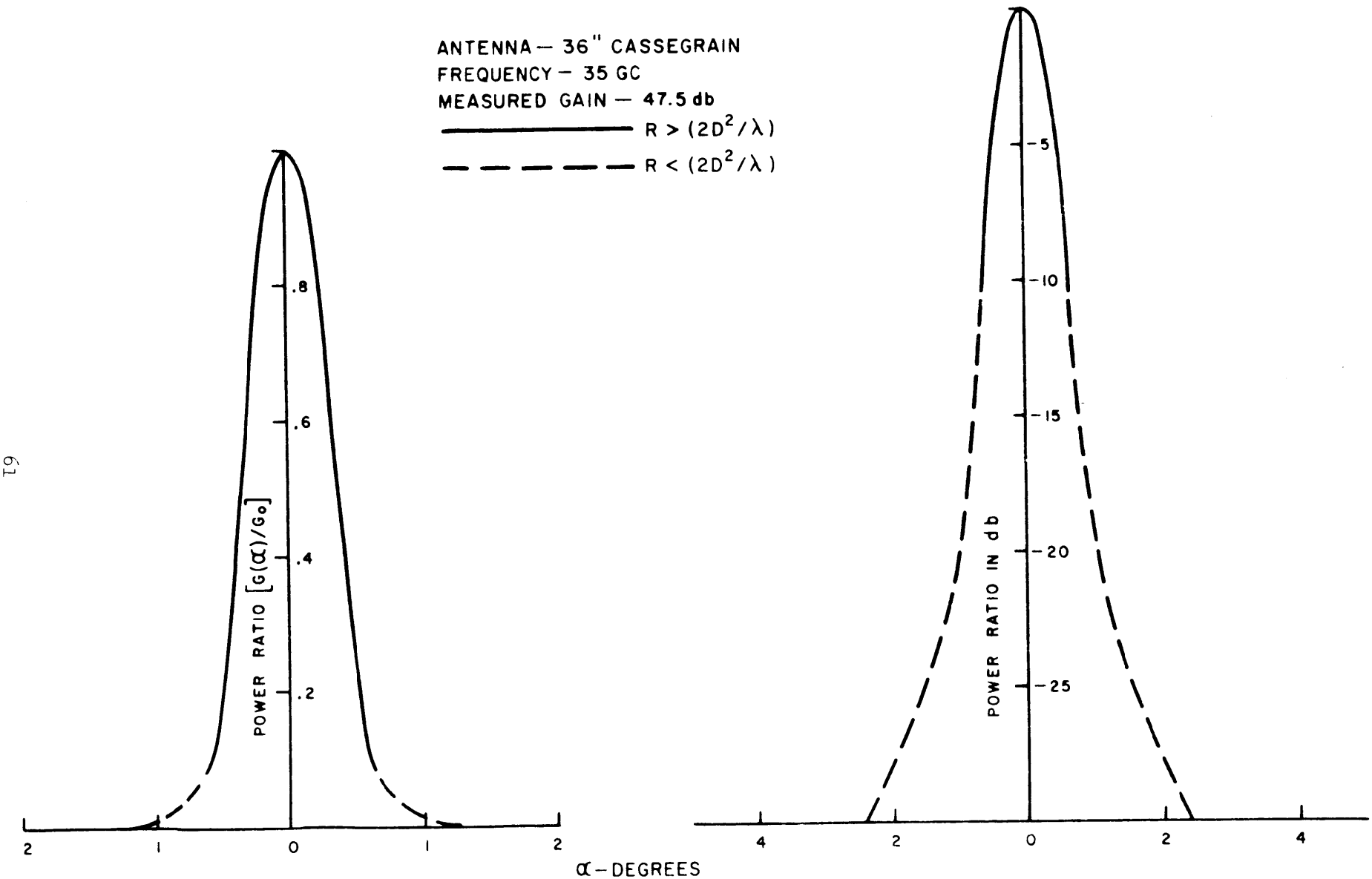

FIGURE 14. NORMALIZED EFFECTIVE POWER PATTERN FOR RUN 5.

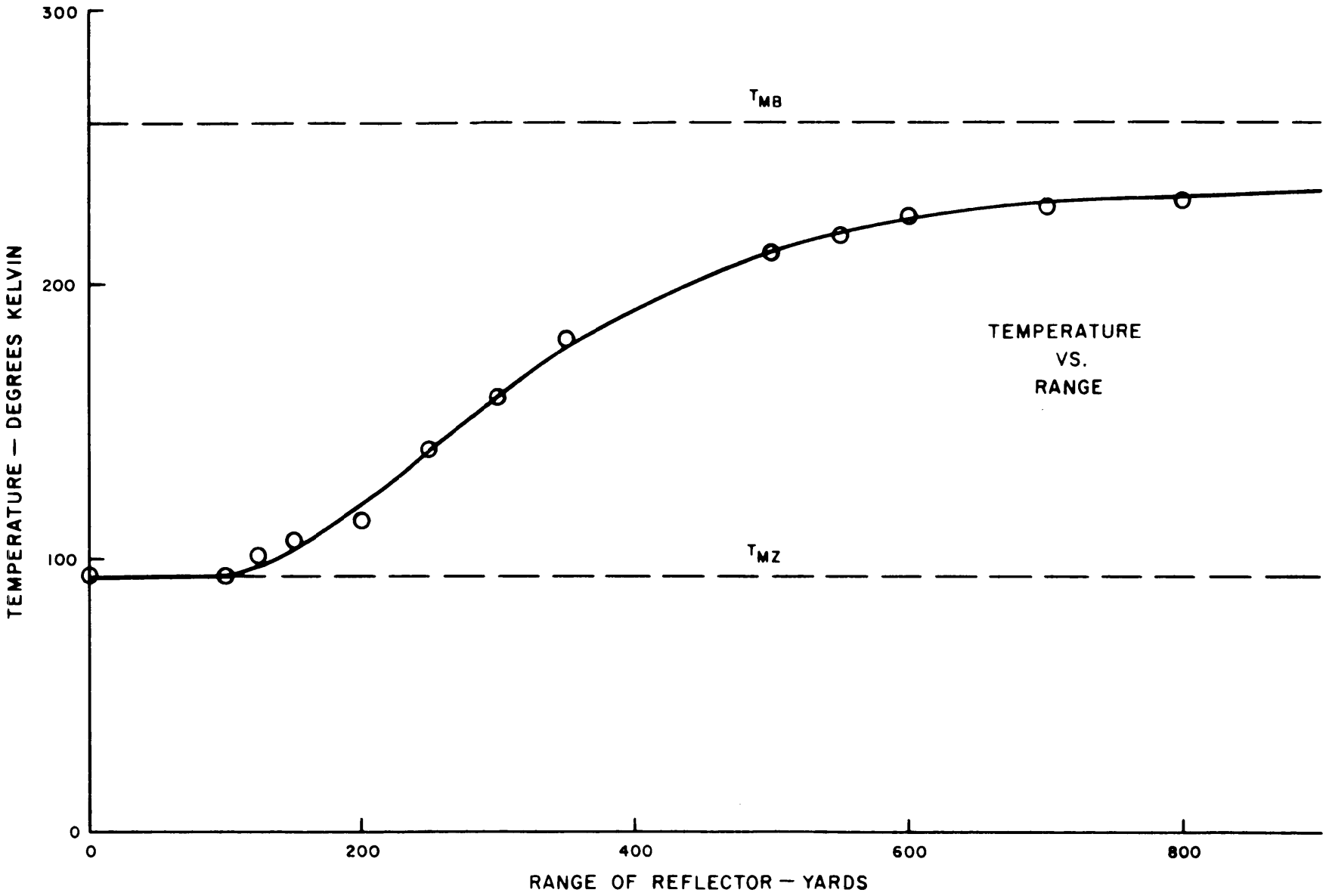

FIGURE 15. MEASURED DATA FOR RUN 6.

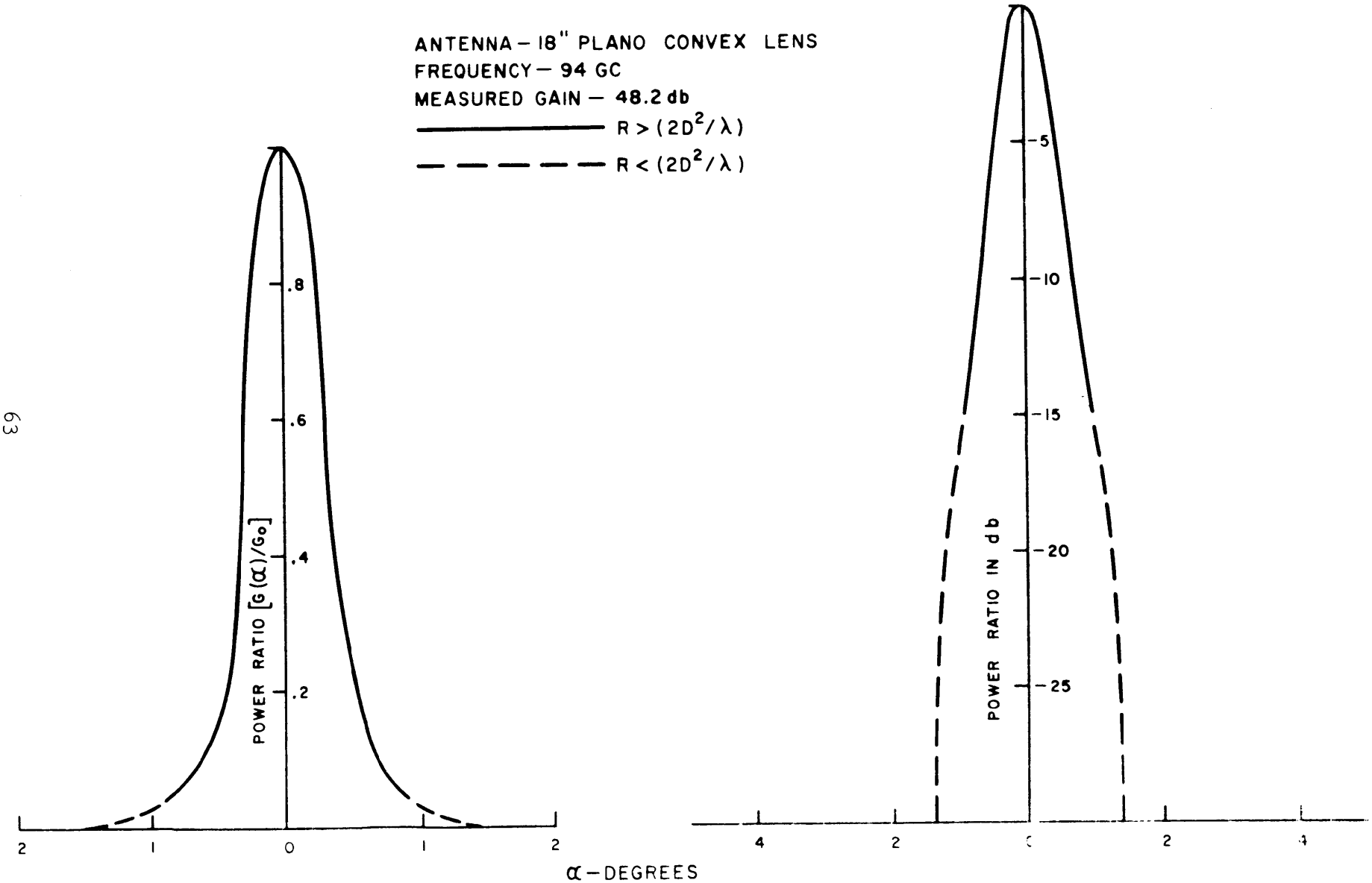

FIGURE 16. NORMALIZED EFFECTIVE POWER PATTERN FOR RUN 6

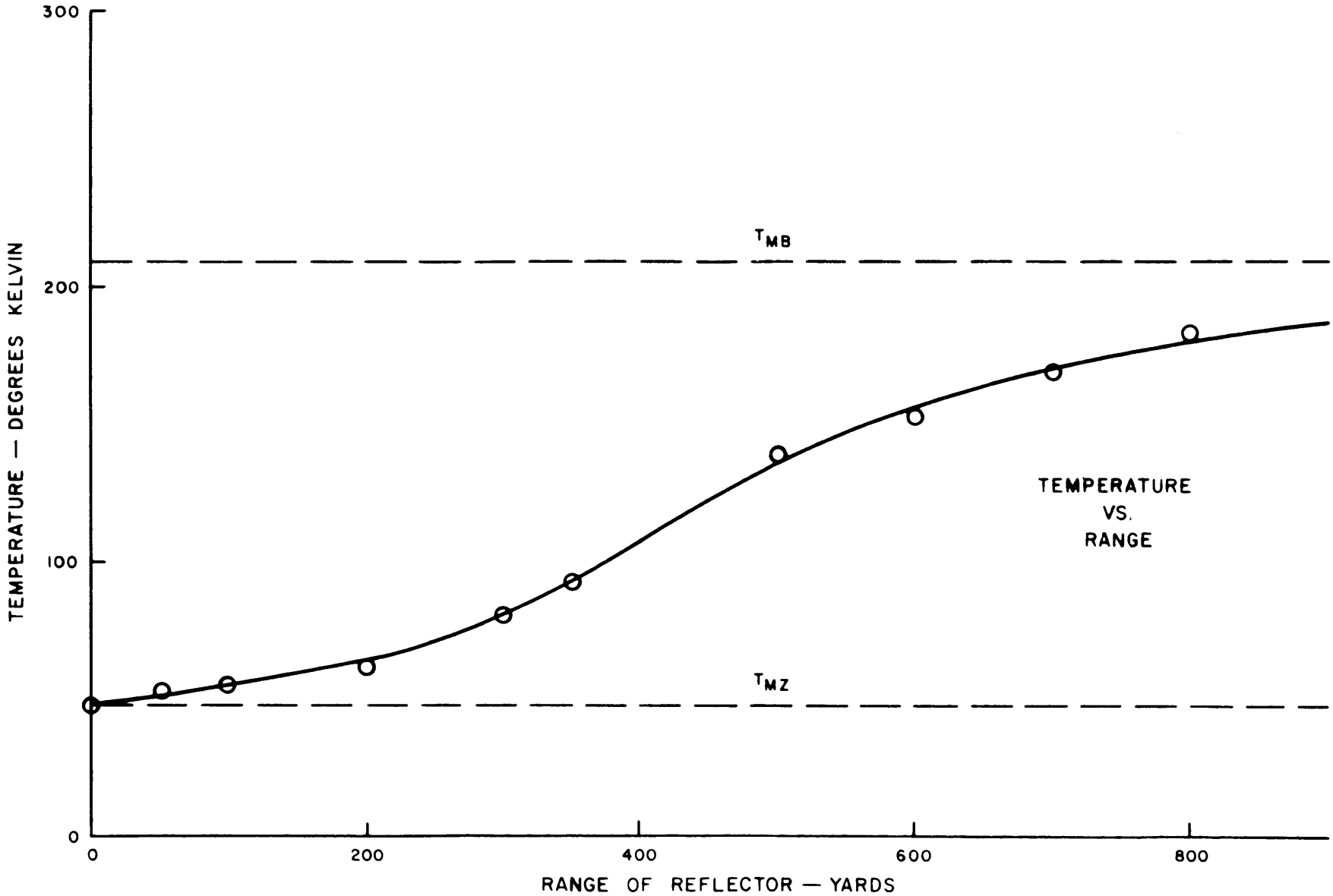

FIGURE 17. MEASURED DATA FOR RUN 7.

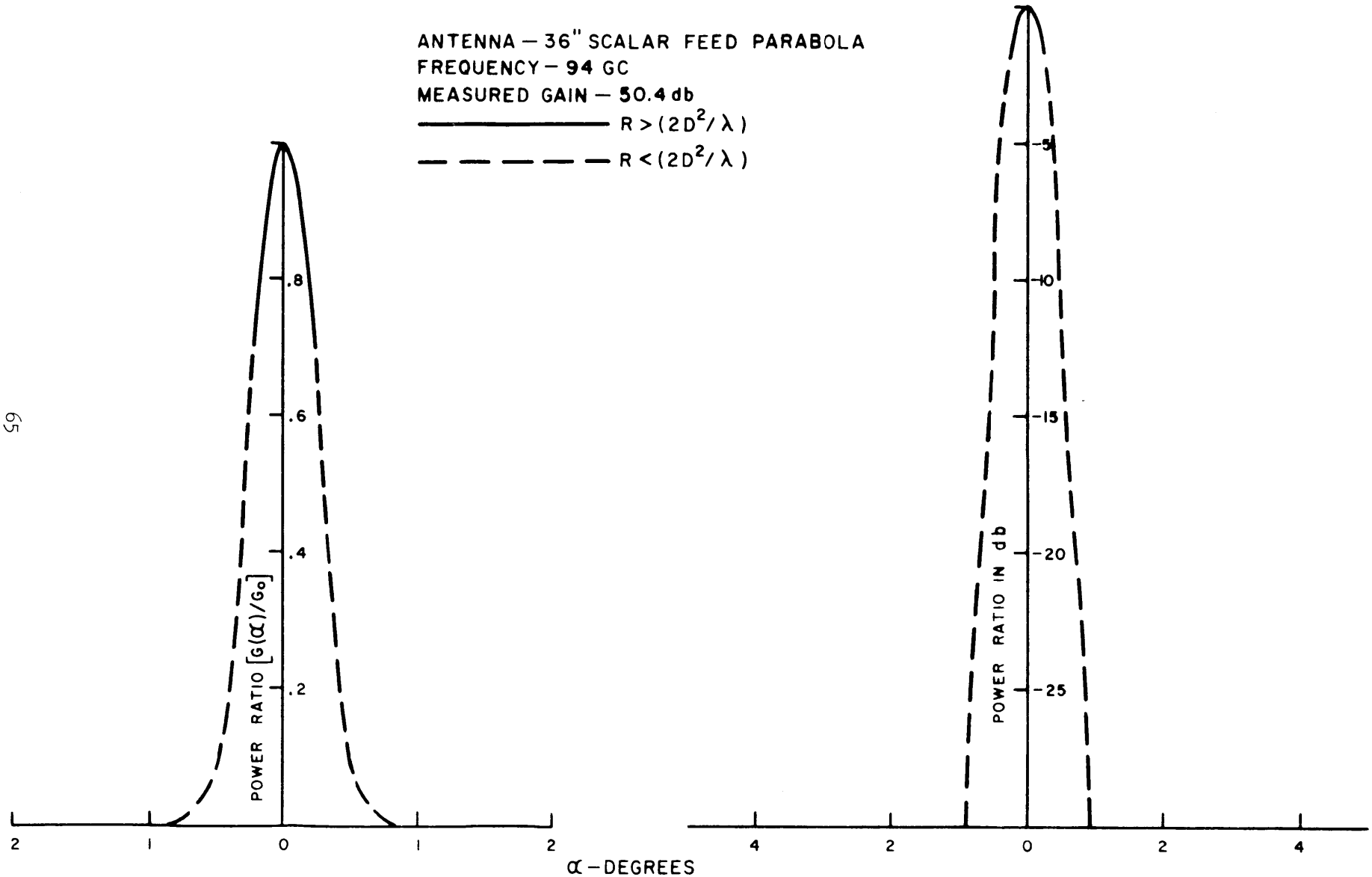

FIGURE 18. NORMALIZED EFFECTIVE POWER PATTERN FOR RUN 7.

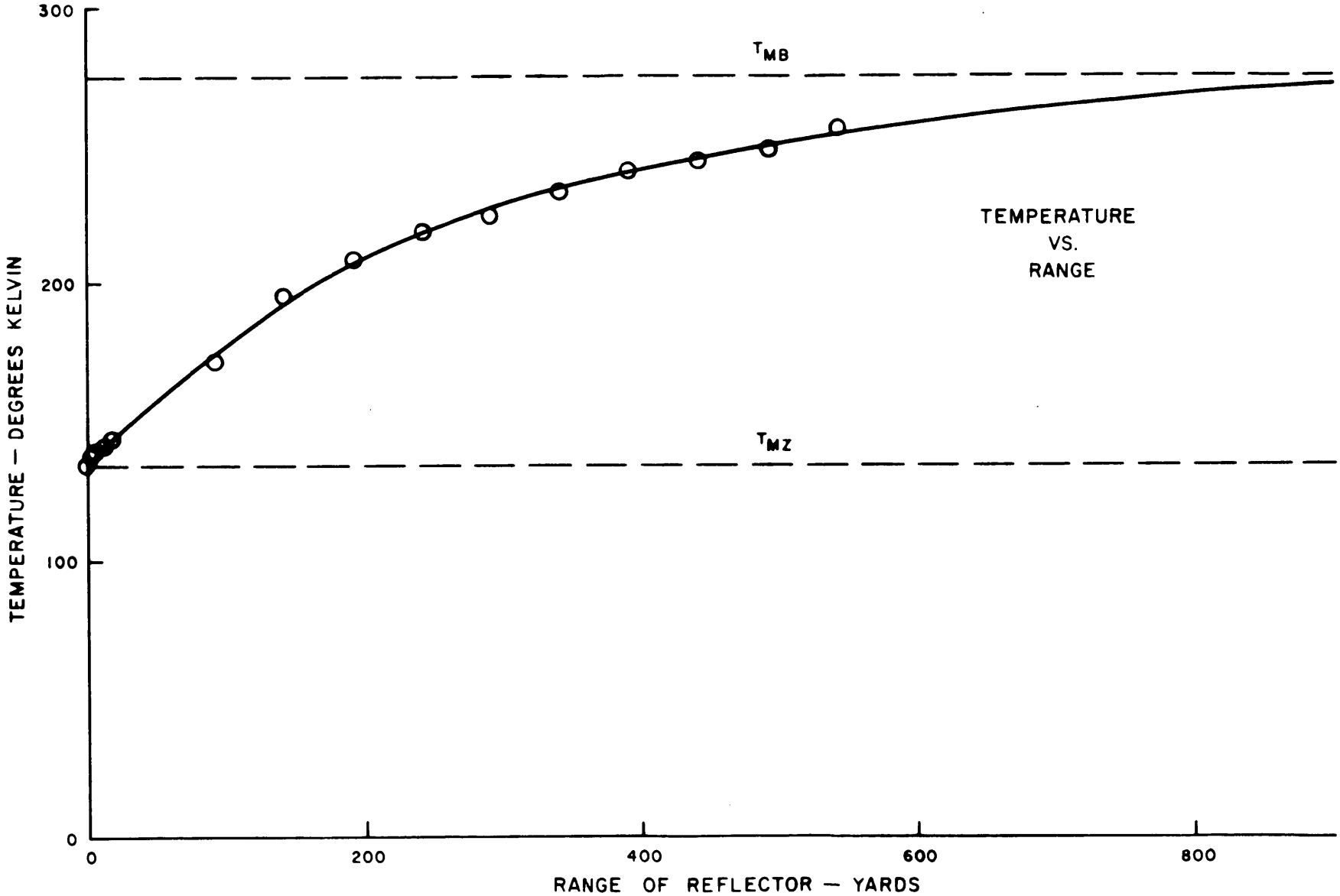

FIGURE 19. MEASURED DATA FOR RUN 8.

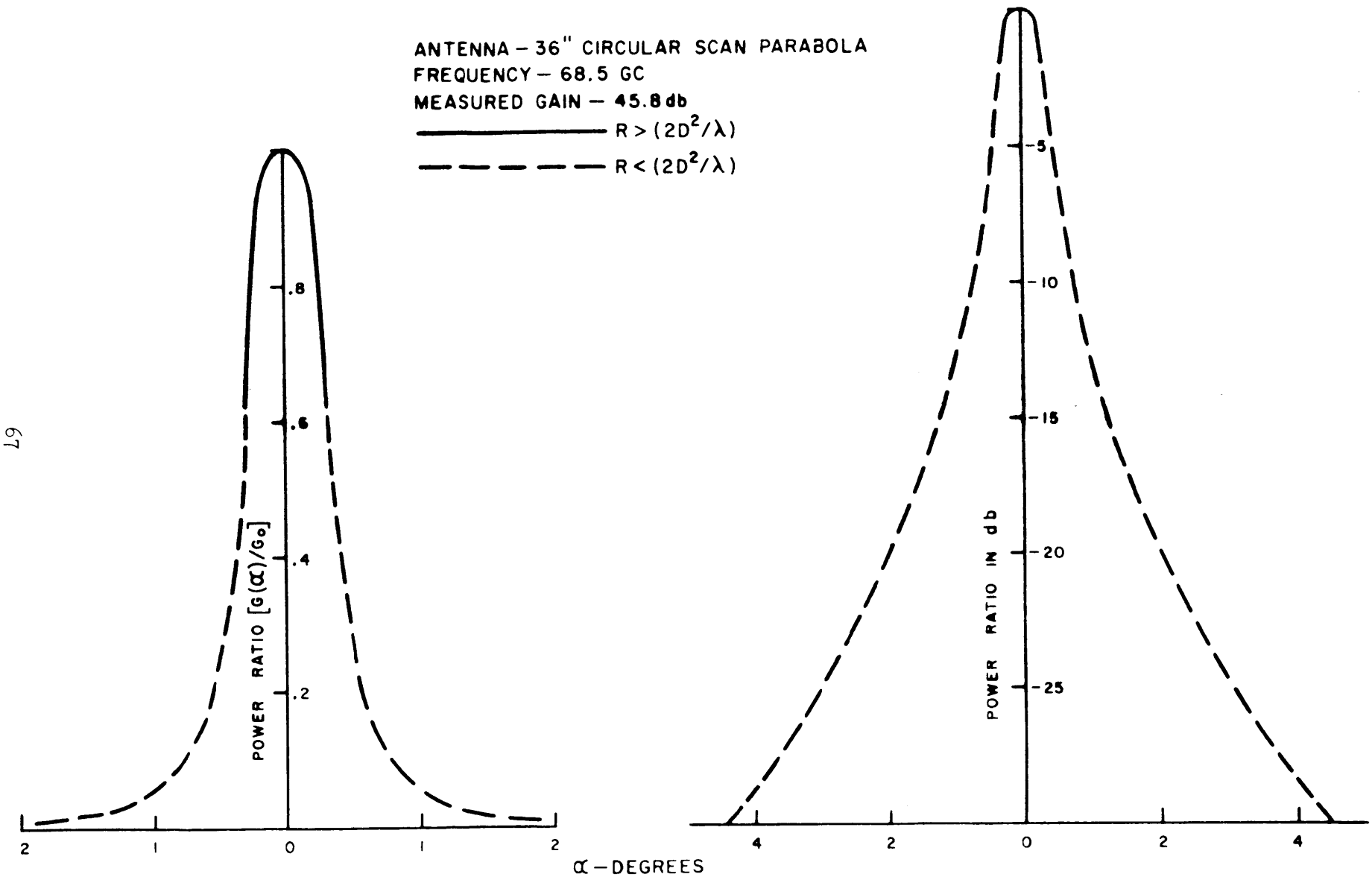

FIGURE 20. NORMALIZED EFFECTIVE POWER PATTERN FOR RUN 8.

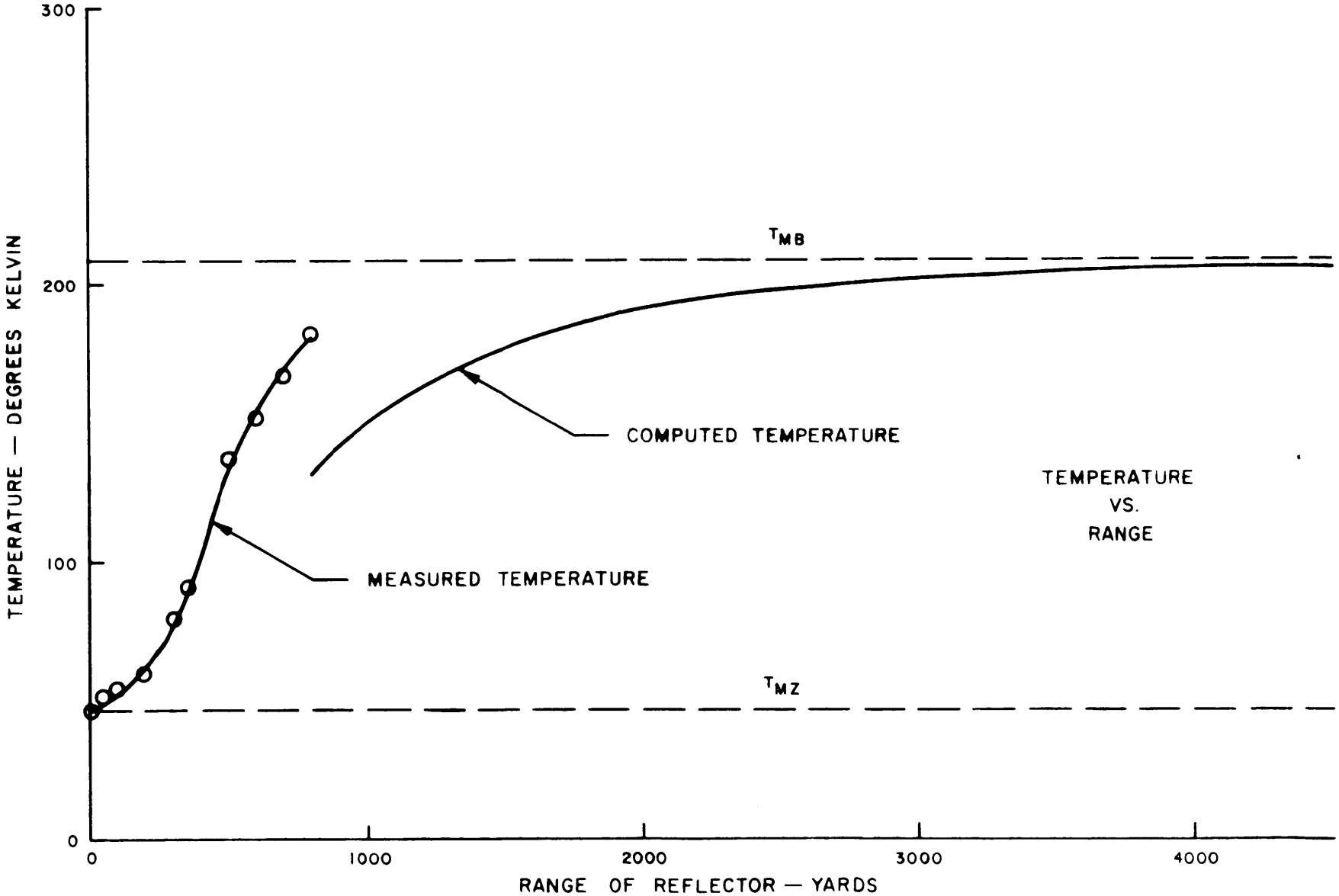

FIGURE 21. COMPARISON OF MEASURED DATA WITH TEMPERATURES COMPUTED FOR ANTENNA WITH 54.2 db GAIN AND 0.24° B.W.

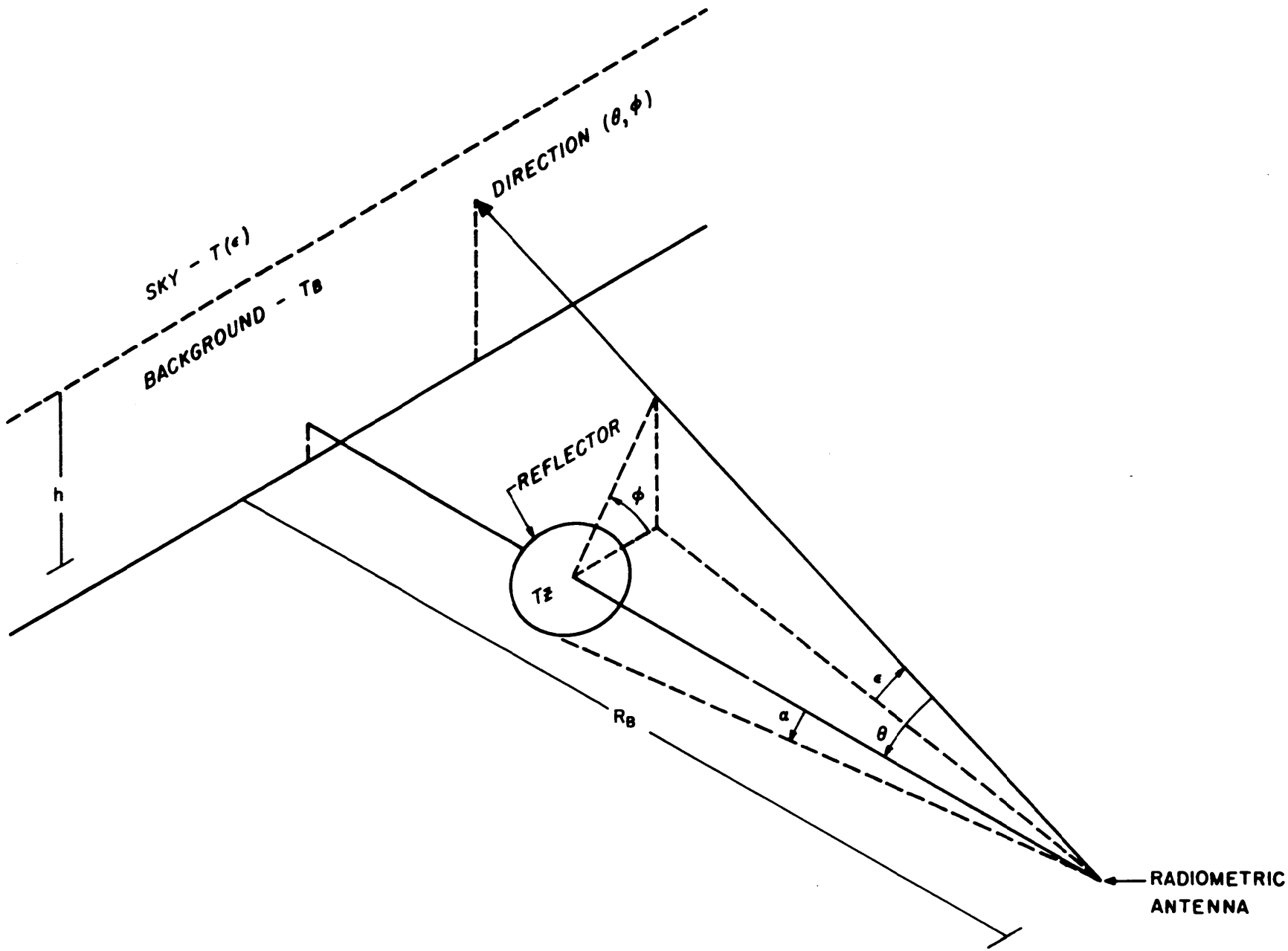

FIGURE 22. VARR SYSTEM GEOMETRY
FOR $\alpha < \tan^{-1}(h/R_B)$

DISTRIBUTION LIST

No. of Copies	Organization
20	Commander Defense Documentation Center ATTN: TIPCR Cameron Station Alexandria, Virginia 22314
1	Director Advanced Research Projects Agency Department of Defense Washington, D.C. 20301
1	Director Institute for Defense Analyses ATTN: Mr. J. W. Sherman, III 400 Army-Navy Drive Arlington, Virginia 22202
1	Director Defense Atomic Support Agency ATTN: STRA(RAEL) LTC Brown Washington, D.C. 20301
1	Director National Security Agency ATTN: Code K-31, Mr. Norvell Fort George G. Meade, Md. 20755
1	Commanding General U.S. Army Materiel Command ATTN: AMCRD-RP-B Washington, D.C. 20315
1	Commanding General U.S. Army Materiel Command ATTN: AMCRD-RP-E Washington, D.C. 20315
1	Commanding General U.S. Army Materiel Command ATTN: AMCRD-DS Washington, D.C. 20315
2	Commanding General U.S. Army Materiel Command ATTN: AMCPM-AI, Mr. Cory Mr. Gardner Washington, D.C. 20315
5	Commanding General U.S. Army Electronics Command ATTN: AMSEL-CB AMSEL-HL-CT-NR AMSEL-RD (2 cys) AMSEL-RD-SRD, Mr. Gelernter Fort Monmouth, N.J. 07703
4	Commanding General U.S. Army Electronics Command ATTN: Dr. Linden Mr. K. Burger Mr. J. McCue AMSEL-RD-NAI, Mr. Berman Fort Monmouth, New Jersey 07703
1	Commanding Officer U.S. Army Electronic Research & Development Activity ATTN: Mr. R. Murray White Sands Missile Range New Mexico 88002
5	Commanding General U.S. Army Missile Command ATTN: AMSMI-RE, Mr. Pittman AMSMI-R Lib AMSMI-RFC (CSS) Mr. Michetti AMSMI-RFE, Mr. Duvall Mr. D. Salonimer Redstone Arsenal, Ala. 35809
1	Director Redstone Scientific Information Center ATTN: Ch, Docu Sec U.S. Army Missile Command Redstone Arsenal, Ala. 35809

DISTRIBUTION LIST

No. of Copies	Organization
4	Commanding Officer U.S. Army Engineer Research & Development Laboratories ATTN: STINFO Div CMEFB-VC, Mr. Hopkins Mr. M. Gale FIB Br, Mr. Crompton Fort Belvoir, Virginia 22060
1	Commanding General U.S. Army Munitions Command Dover, New Jersey 07801
5	Commanding Officer U.S. Army Frankford Arsenal ATTN: N1000, Dr. Lester Mr. Chang Mr. Kerensky Philadelphia, Pa. 19137
1	Commanding Officer U.S. Army Picatinny Arsenal ATTN: FRL Dover, New Jersey 07801
1	Commanding General U.S. Army White Sands Missile Range ATTN: STEWS-TE, Mr. Jose Flores White Sands Missile Range New Mexico 88002
2	Commanding General U.S. Army Weapons Command ATTN: AMSWE-RDF Mr. C. M. Erwin Rock Island, Illinois 61202
1	Commanding Officer U.S. Army Foreign Science & Technology Center Munitions Building, Room 2621 Washington, D.C. 20315
2	Commanding Officer U.S. Army Harry Diamond Laboratories ATTN: AMXDO-RA Mr. Palermo Dr. Saunders Washington, D.C. 20438
3	Commanding Officer U.S. Army Harry Diamond Laboratories ATTN: AMXDO-PP, Mr. Gates AMXDO-RB, Mr. Heinard AMXDO-XA, Mr. Hardin Washington, D.C. 20438
1	Commanding Officer U.S. Army Watertown Arsenal Watertown, Massachusetts 02172
2	Commanding General U.S. Army Combat Developments Command ATTN: CDC3A, Mr. Hardison (1 cy) Fort Belvoir, Virginia 22060
2	Commanding General U.S. Continental Army Command Fort Monroe, Virginia 23351
1	Commanding Officer U.S. Army Radio Propagation Agency ATTN: Mr. S. Perlman Fort Monmouth, New Jersey 07703
1	Commanding General U.S. Army Security Agency ATTN: IALOG/ESE, Mr. C. Craig Arlington Hall Station Arlington, Virginia 22212

DISTRIBUTION LIST

No. of Copies	Organization
1	Commanding Officer U.S. Army Map Service ATTN: Mr. R. Vitek Corps of Engineers 6500 Brooks Lane Washington, D.C. 20315
1	Chief of Research & Development Department of the Army Washington, D.C. 20310
1	Commanding Officer U.S. Army Research Office (Durham) Box CM, Duke Station Durham, North Carolina 27706
5	Chief, Bureau of Naval Weapons ATTN: DLI-3 (3 cys) RAAV-4121 RMWC-421 Mr. C. E. Francis Department of the Navy Washington, D.C. 20360
3	Commanding Officer U.S. Naval Ordnance Laboratory ATTN: Code 454 Mr. H. Johnson Code 45, Mr. F. Essig Code 723, Mr. Lundquist Corona, California 91720
1	Commanding Officer & Director U.S. Navy Electronics Laboratory ATTN: Code 3220C, Mr. B. I. Small San Diego, California 92152
1	Chief, Bureau of Ships ATTN: Code 362A, Mr. R. Fratila Department of the Navy Washington, D.C. 20360
1	Commanding Officer & Director U.S. Navy Underwater Sound Laboratory ATTN: Mr. R. W. Turner Fort Trumbull New London, Connecticut, 06321
4	Director U.S. Naval Research Laboratory ATTN: Code 5250, Dr. Marston Code 5330, Dr. R. Adams Rdo Astron Div Rdr Div Washington, D.C. 20390
3	RADC (EMATA/Mr. Mather Mr. Pankiewicz EMATE/Mr. LaMascola) Griffiss AFB New York 13442
2	AFCRL (CRXLT-1; Ch of Tech Info Div) L. G. Hanscom Fld Bedford, Massachusetts 01731
3	AFCRL (CRD/Mr. Sletten CRDM/Mr. Rotman CRDG/Mr. Blacksmith) L. G. Hanscom Fld Bedford, Massachusetts 01731
1	AFWL (WLL) Kirtland AFB New Mexico 87117
1	USAFSS (Mr. A. Martinez) San Antonio Texas 78241
2	AFAL (AVWW/Mr. Leasure/Mr. Portune) Wright-Patterson AFB Ohio 45433

DISTRIBUTION LIST

No. of Copies	Organization
2	AFAL (AVNT/Mr. Kittering; AVWE/Mr. E. Turner) Wright-Patterson AFB Ohio 45433
1	Director P.O. Box 1925 ATTN: James Casey Washington, D.C. 20505
4	Director U.S. Environmental Science Services Administration ATTN: Code R4, Mr. G. Falcon Mr. G. Lerbold Mr. Cottony Code 425/520.50 Boulder, Colorado 80301
1	Director National Aeronautics & Space Administration Electronics Research Center ATTN: Mwave Radn Lab Mr. Trafford 575 Technology Square Cambridge, Massachusetts 02139
2	Director National Aeronautics & Space Administration Goddard Space Flight Center ATTN: Code 110, Mr. Kampinsky Code 525, Mr. Lantz Greenbelt, Maryland 20771
1	General Dynamics/Pomona ATTN: Mr. W. B. Nash 1675 West Fifth Avenue P.O. Box 2507 Pomona, California 91766
1	University of Michigan The Targets Signature Library ATTN: Mr. J. L. Beard P.O. Box 618 Ann Arbor, Michigan 48104
1	Dr. G. A. Dulk University of Colorado Department of Astro-Geophysics Boulder, Colorado 80304
	Aberdeen Proving Ground
	Ch, Tech Lib
	Air Force Ln Ofc Marine Corps Ln Ofc Navy Ln Ofc CDC Ln Ofc
	CO, USALWL ATTN: Mr. R. Bolgiano Mr. J. Weineg
	Dir, D&PS ATTN: Mr. S. Taragin Mr. A. Kaper

Unclassified
Security Classification

DOCUMENT CONTROL DATA - R&D

(Security classification of title, body of abstract and indexing annotation must be entered when the overall report is classified)

1. ORIGINATING ACTIVITY (Corporate author)	2a. REPORT SECURITY CLASSIFICATION
U.S. Army Ballistic Research Laboratories Aberdeen Proving Ground, Maryland	Unclassified
	2b. GROUP

3. REPORT TITLE

THE VARR METHOD - A TECHNIQUE FOR DETERMINING THE EFFECTIVE POWER PATTERNS OF MILLIMETER-WAVE RADIOMETRIC ANTENNAS

4. DESCRIPTIVE NOTES (Type of report and inclusive dates)

5. AUTHOR(S) (Last name, first name, initial)

Patton, R. B., Jr., and Wilson C. L.

6. REPORT DATE	7a. TOTAL NO. OF PAGES	7b. NO. OF REFS
May 1966	74	1

8a. CONTRACT OR GRANT NO.	9a. ORIGINATOR'S REPORT NUMBER(S)
b. PROJECT NO. RDT&E 1P523801A286	Report No. 1322
c.	9b. OTHER REPORT NO(S) (Any other numbers that may be assigned this report)
d.	

10. AVAILABILITY/LIMITATION NOTICES

Distribution of this document is unlimited.

11. SUPPLEMENTARY NOTES	12. SPONSORING MILITARY ACTIVITY
	U.S. Army Materiel Command Washington, D.C.

13. ABSTRACT

The VARR (VAriable Range Reflector) Method is a technique which has been developed to measure the effective power patterns of millimeter-wave radiometric antennas. In this method, a large movable metallic surface is oriented to reflect radiation from the zenith into an antenna which is directed along the horizontal. Radiometric temperature is measured as a function of the range of the reflector from the antenna. In addition, the water vapor content of the atmosphere and the radiometric temperatures in the directions of background and zenith are observed.

A computing procedure has been devised to determine the complete pattern and gain characteristics of the antenna system purely on the basis of data provided by the measuring system. The method has been used to successfully determine the effective power patterns of a number of antenna systems. These results form the basis of a comparative evaluation of antenna system performance that is in substantial agreement with the observed effectiveness of these same antennas in previous measurements.

DD FORM 1 JAN 64 1473

Unclassified
Security Classification

14. KEY WORDS	LINK A		LINK B		LINK C	
	ROLE	WT	ROLE	WT	ROLE	WT
Radiometric Antennas Power Pattern Determination Radiometric Temperature Measurement Data Reduction						

INSTRUCTIONS

1. ORIGINATING ACTIVITY: Enter the name and address of the contractor, subcontractor, grantee, Department of Defense activity or other organization *(corporate author)* issuing the report.

2a. REPORT SECURITY CLASSIFICATION: Enter the overall security classification of the report. Indicate whether "Restricted Data" is included. Marking is to be in accordance with appropriate security regulations.

2b. GROUP: Automatic downgrading is specified in DoD Directive 5200.10 and Armed Forces Industrial Manual. Enter the group number. Also, when applicable, show that optional markings have been used for Group 3 and Group 4 as authorized.

3. REPORT TITLE: Enter the complete report title in all capital letters. Titles in all cases should be unclassified. If a meaningful title cannot be selected without classification, show title classification in all capitals in parenthesis immediately following the title.

4. DESCRIPTIVE NOTES: If appropriate, enter the type of report, e.g., interim, progress, summary, annual, or final. Give the inclusive dates when a specific reporting period is covered.

5. AUTHOR(S): Enter the name(s) of author(s) as shown on or in the report. Enter last name, first name, middle initial. If military, show rank and branch of service. The name of the principal author is an absolute minimum requirement.

6. REPORT DATE: Enter the date of the report as day, month, year; or month, year. If more than one date appears on the report, use date of publication.

7a. TOTAL NUMBER OF PAGES: The total page count should follow normal pagination procedures, i.e., enter the number of pages containing information.

7b. NUMBER OF REFERENCES: Enter the total number of references cited in the report.

8a. CONTRACT OR GRANT NUMBER: If appropriate, enter the applicable number of the contract or grant under which the report was written.

8b, 8c, & 8d. PROJECT NUMBER: Enter the appropriate military department identification, such as project number, subproject number, system numbers, task number, etc.

9a. ORIGINATOR'S REPORT NUMBER(S): Enter the official report number by which the document will be identified and controlled by the originating activity. This number must be unique to this report.

9b. OTHER REPORT NUMBER(S): If the report has been assigned any other report numbers *(either by the originator or by the sponsor)*, also enter this number(s).

10. AVAILABILITY/LIMITATION NOTICES: Enter any limitations on further dissemination of the report, other than those imposed by security classification, using standard statements such as:

(1) "Qualified requesters may obtain copies of this report from DDC."

(2) "Foreign announcement and dissemination of this report by DDC is not authorized."

(3) "U. S. Government agencies may obtain copies of this report directly from DDC. Other qualified DDC users shall request through _____."

(4) "U. S. military agencies may obtain copies of this report directly from DDC. Other qualified users shall request through _____."

(5) "All distribution of this report is controlled. Qualified DDC users shall request through _____."

If the report has been furnished to the Office of Technical Services, Department of Commerce, for sale to the public, indicate this fact and enter the price, if known.

11. SUPPLEMENTARY NOTES: Use for additional explanatory notes.

12. SPONSORING MILITARY ACTIVITY: Enter the name of the departmental project office or laboratory sponsoring *(paying for)* the research and development. Include address.

13. ABSTRACT: Enter an abstract giving a brief and factual summary of the document indicative of the report, even though it may also appear elsewhere in the body of the technical report. If additional space is required, a continuation sheet shall be attached.

It is highly desirable that the abstract of classified reports be unclassified. Each paragraph of the abstract shall end with an indication of the military security classification of the information in the paragraph, represented as *(TS)*, *(S)*, *(C)*, or *(U)*.

There is no limitation on the length of the abstract. However, the suggested length is from 150 to 225 words.

14. KEY WORDS: Key words are technically meaningful terms or short phrases that characterize a report and may be used as index entries for cataloging the report. Key words must be selected so that no security classification is required. Identifiers, such as equipment model designation, trade name, military project code name, geographic location, may be used as key words but will be followed by an indication of technical context. The assignment of links, rules, and weights is optional.